JOURNAL OF MATERIALS SCIENCE **34** (1999) 4671–4697

Effect of Mg on the ageing behaviour of Al-Si-Cu 319 type aluminium casting alloys

P. OUELLET, F. H. SAMUEL
Département des Sciences Appliquées, Université du Québec à Chicoutimi, Chicoutimi, Québec, Canada G7H 2B1
E-mail: fhsamuel@uqac.uquebec.ca

The present study was performed on primary A319.2 alloy to investigate the effect of magnesium addition as well as other melt treatment parameters such as Sr modification and grain refinement on the heat treatment behaviour of the alloy. The results show that increasing the Mg content in A319.2 up to 0.45% considerably enchances the alloy response to heat treatment in the T5 and T6 tempers, more particularly, the T6 temper. Modification of the high-Mg version of 319 alloy with Sr in amounts of ~350 ppm results in a marked amount of porosity formation which counteracts the beneficial effect of the modification, leading to a noticeable decline in the alloy strength. Grain refining the Sr-modified (A319.2 + 0.45% Mg) alloy produces sounder castings and, hence, an identical ageing response to that offered by unmodified high-Mg alloys. The properties, however, are more consistent. Addition of Mg (~0.45%) leads to the precipitation of coarse particles of $Al_5Mg_8Si_6Cu_2$. Modification with Sr tends to cause severe segregation of both Cu-containing intermetallics, i.e., Al_2Cu and $Al_5Mg_8Si_6Cu_2$ in areas away from the growing Al-Si eutectic regions. Thus, their dissolution rates are fairly sluggish upon solutionizing at 505 °C. Increasing the solutionizing temperature would lead to incipient melting of the phases and, hence, a catastrophic failure. Fracture of intermetallic phases in the interdendritic regions is mostly brittle, with the formation of microcracks at the Si, Cu, Fe-base intermetallics and aluminium interfaces. Fracture of the α-aluminium is always ductile. Hardening during ageing occurs by cooperative precipitation of Al_2Cu and Mg_2Si phase particles.

1. Introduction

Although an extensive amount of information is available on the heat treatment of Al-Si-Mg alloys, not much data, however, is published on the heat treatment of 319 type Al-Si-Mg Si-Cu alloys. Beumler *et al.* [1] have reported that the mechanical properties of 319 alloy depend on the alloy structure, i.e., modified or unmodified.

A series of investigations was carried out by Das-Gupta *et al*. [2–4] to study the effect of an increased Mg content (from 0.07 to 0.54%) on the mechanical properties of sand and permanent mold cast aluminum alloys. Their results show that increasing the Mg content has a negligible effect on the alloy mechanical properties. Futhermore, no significant microstructural changes occur either in the as-cast or in the T5 conditions.

An intensive research program on the treatment of 319 type alloys was undertaken at the Université du Québec à Chicoutimi to determine the optimum solution heat treatment parameters with respect to the alloy Mg level [5–6]. The results indicated that for alloys containing very low concentrations of Mg i.e., 0.06%, fluctuations in solution temperature should be controlled within a very narrow range, due to the presence of the low-melting point Al_2Cu phase. Also, the optimum solution heat treatment parameters with respect to the alloy ductility may be achieved through a two-step solution heat treatment, in which case, the alloy would be heated for another 8 h at 540 °C prior to quenching in hot water [7].

For high Mg-containing alloys, however, a single-step solution treatment consisting of solutionizing at 505 °C for 12 h would be recommended. This process should be followed by artificial ageing for 2–5 h at 158 °C. Overageing does not bring about much change in the tensile properties [5].

Based on calculations of the quality index (Q) for each solution time for the A319.2 alloy (~0.06% Mg), a general from was proposed by Gauthier *et al*. [8] for the temperature range 480–515 °C:

$$Q\,(\text{MPa}) = UTS\,(\text{MPa}) + 124 \log EL$$

which is very close to that proposed for A356 alloy [9]. Gauthier *et al*. [7–8] also found that peak ageing was attained after 24 h at 155 °C or 5 h at 180 °C. The associated tensile properties were 253 MPa (*YS*), 403 MPa (*UTS*) and 1.2% elongation. In the T4 temper condition, the A319.2 alloy exhibited 200 MPa (*YS*), 320 MPa (*UTS*), and 3.7% elongation.

TABLE I Suggested heat treatments for 319 type alloys—permanent mould casting [18]

Heat treatment	Description
T5	Ageing for 7–9 h at 205 °C, air cooling to room temperature.
T6	Solutionizing for 8 h at 510 °C, quenching in hot water (60 °C), ageing for 2–5 h at 158 °C, air cooling to room temperature.

Table I describes the T5 and T6 heat treatments recommended for 319 permanent mould castings by the Aluminium Association. The work of Crepeau *et al*. [10] on T5 treatment of 339 alloy shows the cooperative precipitation of Al_2Cu and Mg_2Si phases which are responsible for alloy hardening. The effectiveness of this process depends chiefly on the solidification rate of the casting [11]. Permanent mould castings would retain an appreciable amount of Mg and Cu in solid solution. During ageing, these two elements precipitate in the form of a large proportion of fine particles, which, in turn render the alloy its strength.

Shivkumar *et al*. [12] have studied the parameters that control the tensile properties of A356 alloy in the T6 temper. The improvement in the alloy strength has been attributed to the precipitation of negligible phases from a supersaturated matrix. The sequence of precipitation in Al-Si-Mg alloys could be described as follows:

(i) precipitation of GP zones (needles about 10 nm long);
(ii) intermediate phase β'-Mg_2Si, (homogeneous precipitation);
(iii) intermediate phase β'-Mg_2Si, (heterogeneous precipitation);
(iv) equilibrium phase β-Mg_2Si, fcc structure ($a = 0.639$ nm), rod or plate-shaped ($0.1 \times 1\,\mu$m).

The maximum alloy strength (peak-ageing) is achieved just before the precipitation of the incoherent β-platelets.

Apelian *et al*. [13] have studied the ageing behaviour of Al-Si-Mg alloys. The precipitation of very fine β' (Mg_2Si) during ageing leads to a pronounced improvement in strength properties. Both ageing time and temperature determine the final properties. It has been established that increasing the ageing temperature by 10 °C is equivalent to increasing the ageing time by a factor of two. When Cu is added to the Al-Si-Mg system, precipitation of fine θ (Al_2Cu) is expected to take place, which contributes further to the alloy strength parameters i.e. *YS* and *UTS*. Elongation is expected to show an opposite trend.

Most of the recommended heat treatments for Al-Si alloys restrict solution temperature below the final solidification point in order to avoid the melting of Cu-containing phases. One equilibrium heat treatment was suggested by Awano and Shimizu [14] for an Al-7% Si-3% Cu alloy. This treatment involves solutionizing at a temperature slightly higher than the final solidification of the ($Al + Al_2Cu$) eutectic. This process is expected to enhance dissolution of Al_2Cu in the Al matrix.

The work of DasGupta *et al*. [4] on the fracture behaviour of A356 alloy as a function of modification level shows that unmodified samples exhibit essentially a brittle fracture. This brittle mode of fracture is attributed to the presence of a plate/rod-like silicon eutectic structure. Gangulee and Gurland [15] have shown that fracture in Al-Si alloys occurs in three stages:

(a) crack initiation of the Si particles;
(b) propagation of crack in the interdendritic regions; and
(c) rupture of the matrix.

The interdendritic regions have been observed by Crepeau *et al*. [10] to fail first. Dendritic cells on the fracture surface form ligaments that become aligned in the loading direction and necked to pinpoints. The microstructure analysis reported by Pan *et al*. [16] indicates that cracks are prone to initiate and propagate along the coarse and flaky eutectic silicon phase particles that are present in the unmodified alloy. The fracture mode, in general, is characterized by a microvoid coalescence dimpled rupture.

A metallographic study was carried out by Samuel and Samuel [17] on porosity and fracture behaviour in unidirectionally solidified end-chill castings of unmodified 319.2 aluminium alloy. Under tensile loading, fracture of Si, β-Al_5FeSi, α-$Al_{15}(Fe, Mn)_3Si_2$ and Al_2Cu phases was observed to take place within the phase particles rather than at the particle/Al matrix interface, the ductile matrix resisting crack propagation. This process was independent of the solidification parameters or alloy chemistry.

The present study was undertaken to investigate the effect of increasing the Mg content up to 0.45% on the tensile properties of primary 319.2 alloys in T5 and T6 tempers, over a wide range of ageing temperatures (150–250 °C). It was also carried out to determine the relationship between the tensile properties of heat-treated test bars (possessing the two levels of Mg) and their fracture characteristics.

2. Experimental

The chemical composition of the as-received alloy (coded G alloy) is given in Table II. The supplied ingots (12.5 kg) were cut, dried, and melted in a silicon carbide crucible of 30 kg capacity, using an electrical resistance furnace. The melting temperature was held at 735 ± 5 °C. At this temperature, measured amounts of Mg (as pure metal) and Sr (as Al-10% Sr master alloy) were added. The molten metal was degassed using pure dry argon, which was injected into the melt using

TABLE II Chemical composition (wt %) of primary alloys

Alloy code	Si	Cu	Fe	Mg	Mn	Ti	Zn	Sr
G	6.23	3.77	0.46	0.06	0.14	0.13	0.08	—
GM	6.23	3.77	0.46	0.46	0.14	0.13	0.08	—
GMS	6.23	3.77	0.46	0.45	0.14	0.13	0.08	0.038
GMST	6.23	3.77	0.46	0.43	0.14	0.13	0.08	0.041

a graphite impeller rotating at 150 rpm. In all cases, the hydrogen level was less than 0.1 ml/100 g Al (as measured by an AlScan^{TM} apparatus). The molten metal was then poured into a Stahl permanent mould (type ASTM B-108) heated at 420 °C. Samples for chemical analysis were also taken for each pouring. Actual Mg and Sr concentrations and the respective alloy codes are also shown in Table II.

Test bars obtained from the Stahl mould casting were solutionized in an air-forced furnace at 500 °C for 8 h, followed by quenching in hot water (∼80 °C). The as-cast and the solutionized test bars were aged in the temperature range of 150–250 °C for times ranging between 0 and 48 h. In each case, 6 test bars was used. The T5 and T6-treated test bars were pulled to fracture in an Instron universal testing machine at a strain rate of 4×10^{-4}/s. A strain gauge extensometer (2 in range) was attached to the test bars for measuring the alloy ductility. Mechanical properties, namely, yield strength (*YS*) at 0.2% offset strain, ultimate tensile strength (*UTS*), and fracture elongation (*El* %), were derived from the data acquisition system of the machine.

Microstructural changes were examined using optical microscopy on polished sample surfaces of specimens obtained from the fractured test bars. These specimens were cut from the gauge length, normal to the loading axis and away from the plastic deformation zone. Fracture surfaces of the tensile test bars were examined using a scanning electron microscope equipped with an EDX system for element analysis. In addition, samples taken from longitudinal sections passing through the fractured surface were polished and examined to study the extent of damage beneath the fracture surface.

3. Results and discussion

3.1. Tensile properties

For each alloy composition, a sum of 400 test bars were cast into final form. Six test bars were chosen randomly for X-ray examination to determine the type and intensity of casting/solidification defects. Most of the G alloy test bars were sound with negligible gas porosity (rated "slight" according to ASTM standards). Addition of Mg up to 0.45% did not cause any particular type of casting defects, especially when the molten metal was properly degassed using a rotary impeller running at speeds as high as 150 rpm. Modification with Sr, on the other hand, resulted in the presence of a large volume fraction of porosity in at least 50% of the total number of test bars. Grain refining of Sr-modified high Mg-containing alloys led to sounder castings with finer grain sizes.

3.2. T5 treatment

3.2.1. Yield strength

The yield strength (*YS*) of G alloy in the as-cast condition, Fig. 1a, is about 140 MPa. Ageing at 150 °C reveals a reduction in *YS* for ageing times of 4–16 h, followed thereafter by a continuous increase up to 48 h. The maximum attainable *YS* at this temperature is ∼185 MPa. Test bars aged for times varying between 0 and 16 h at 180, 200, and 220 °C produced more or less the same levels of *YS*. Beyond 16 h, ageing at 200 and 220 °C showed a marked decrease in the *YS* compared to values obtained at 180 °C. Ageing at 250 °C, however, was associated with an almost immediate softening, reaching 127 MPa after 48 h.

Modification of the GM alloy with Sr, i.e. GMS alloy, does not seem to exert significant changes in the alloy behaviour upon ageing (Fig. 3a). Maximum hardening ∼219 MPa was obtained when the alloy was aged either for 48 h at 150 °C or at 200 °C. It is interesting to note that ageing at 180 and 200 °C results in a substantial increase in *YS* up to 16 h (∼200 MPa), followed thereafter by a steady state period that lasted up to 48 h. Over-ageing was evident when the alloy was aged at 250 °C, leading to a value close to 120 MPa.

The combined effect of modification and grain refining on the ageing behaviour of GM alloy, i.e., GMST is shown in Fig. 4a. In the as-cast condition, the *YS* was about 164 MPa. This value increased up to 248 MPa upon ageing at 200 and 220 °C, peak-ageing (236 MPa) being observed after 4 h. Further increase in the ageing temperature, i.e., 250 °C led to a continuous softening, similar to that reported for the other alloys.

3.2.2. Ultimate tensile strength

The *UTS* of the alloy G in the as-cast condition is about 218 MPa (Fig. 1b). As can be seen, the alloy exhibited a slight decrease in *UTS* in the initial stages of ageing in the temperature range 150–220 °C for times up to 8 h. The maximum attainable level of *UTS* (234 MPa) was achieved after ageing for 24 h at 180 °C. Ageing at temperatures as high as 250 °C led to softening with a minimum *UTS* value of the order of 189 MPa after 16 h.

The addition of 0.45% Mg, i.e., GM alloy resulted in a slight increase in the *UTS* of the as-cast test bars ∼227 MPa. The effect of Mg addition was more pronounced when the alloy was aged at 150 °C, where continuous hardening with ageing time was the main observation (Fig. 2b). At 180 °C, the maximum *UTS* ∼259 MPa was achieved after 16 h. At 200 °C, the alloy hardened during the initial ageing period, where the *UTS* did not show much change. The steady-state behaviour was more obvious when the alloy was aged at 220 °C and continued up to 48 h. Further increase in the ageing temperature, i.e., 250 °C, led to alloy softening.

The GMS alloy (0.45% Mg + 0.04% Sr) exhibited unexpected variations in *UTS* values upon ageing, as shown in Fig. 3b. Ageing at 150, 180, 200 °C produced more or less the same levels of *UTS* up to 16 h. Thereafter, a continuous hardening was observed at 150 °C, whereas the *UTS* remained almost constant at 180 and 200 °C. It should be noted here that ageing at 180 and 200 °C resulted in similar values of *UTS*. Also, softening started at 220 °C and further at 250 °C. It should be borne in mind that the GMS alloy contained a fairly large amount of porosity, as was confirmed by X-ray radiography.

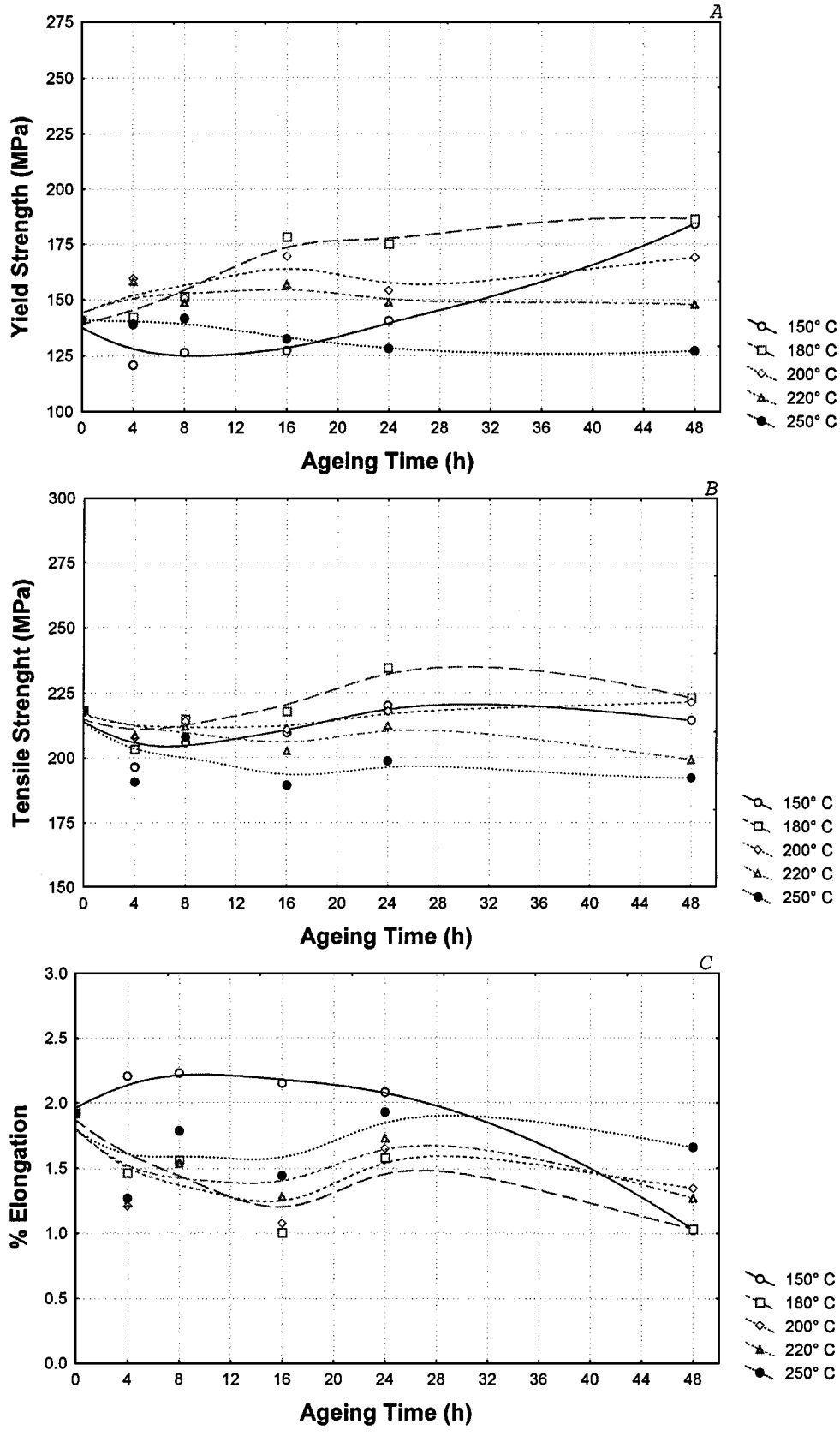

Figure 1 Variation in the tensile properties of G alloy in the T5 condition: (a) *YS*, (b) *UTS*, and (c) % *El*.

The modified grain-refined alloy (GMST) revealed a greater response to ageing compared to GMS alloy, as shown in Fig. 4b. The alloy hardened continuously at 150 °C, reaching a *UTS* value ∼253 MPa after 48 h. At 180 °C, the alloy exhibited a steep hardening up to 18 h, followed by a steady-state (plateau) period. Ageing at 200 and 220 °C were characterized by the presence of peak-ageing at *UTS* levels of 253 and 230 MPa, respectively, followed by over-ageing stages. As expected, ageing at 250 °C led to immediate over-ageing.

3.2.3. % Elongation

Fig. 1c depicts the variation in % elongation of G alloy as a function of ageing temperature and time. The

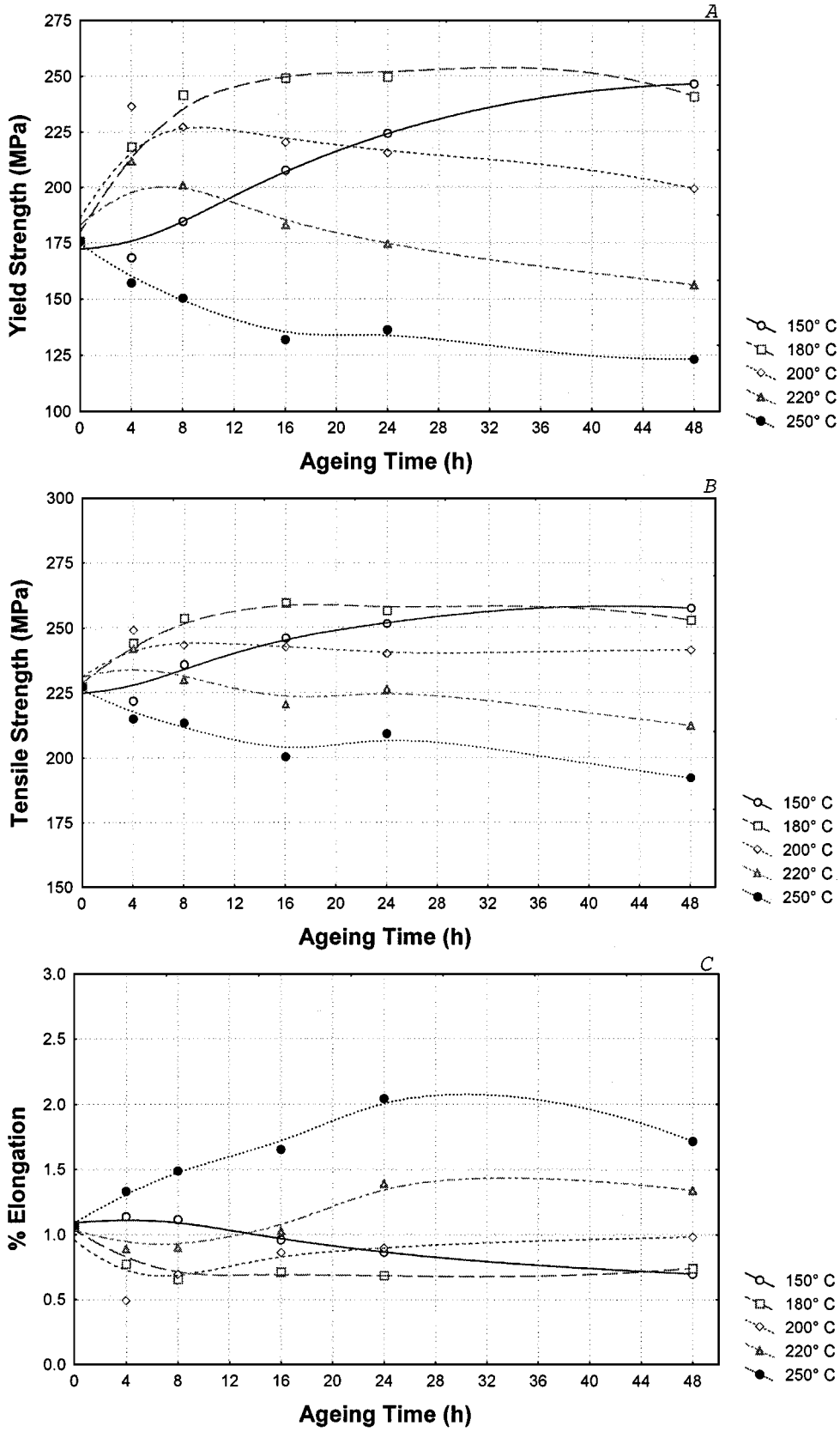

Figure 2 Variation in the tensile properties of GM alloy in the T5 condition: (a) *YS*, (b) *UTS*, and (c) % *El*.

as-cast value is about 1.92%. The initial softening reported in Fig. 1a and b was associated with an increase in the alloy ductility, reaching a value close to 2.2% after ageing for 8 h at 150 °C. With the increase in ageing time at this temperature, the ductility decreased up to 48 h. Ageing at temperatures in the range 180–250 °C showed an opposite behaviour. The minimum attainable ductility, as inferred from Fig. 1c, was about 1%, corresponding to ageing for 16 h at 180 °C.

The addition of Mg in amounts of 0.45% resulted in reducing the as-cast % elongation to unity. Ageing in the temperature range of 150–220 °C further reduced the alloy ductility (0.7%). Increasing the ageing time, 24 h at 220 °C, however, enhanced the alloy

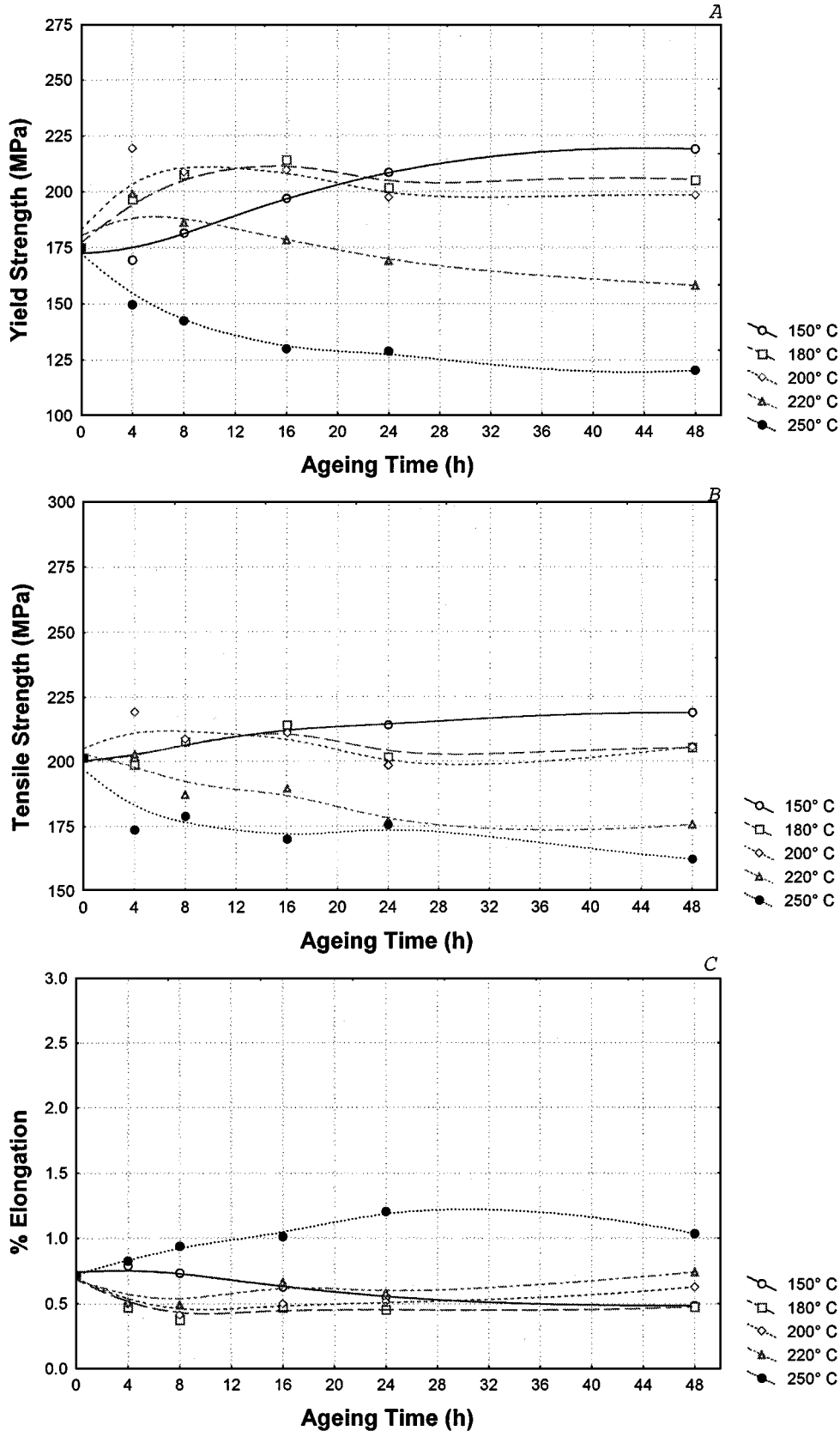

Figure 3 Variation in the tensile properties of GMS alloy in the T5 condition: (a) *YS*, (b) *UTS*, and (c) % *El*.

% elongation (∼1.4%). As expected, ageing at 250 °C contributed significantly to alloy ductility (∼2.1%, 24 h).

The dependence of ductility (as measured by % elongation up to the rupture point) on ageing conditions for GMS alloy is shown by the plots in Fig. 3c. Due to the presence of porosity, the as-cast value is ∼0.22%. It is evident from Fig. 3c that ageing at a low temperature, i.e., 150–220 °C, diminishes the elongation to less than 0.4%. Improvement in the alloy % elongation only occurs when the alloy is aged at 250 °C. Even after 24 h, the maximum attainable elongation is about 1.2%.

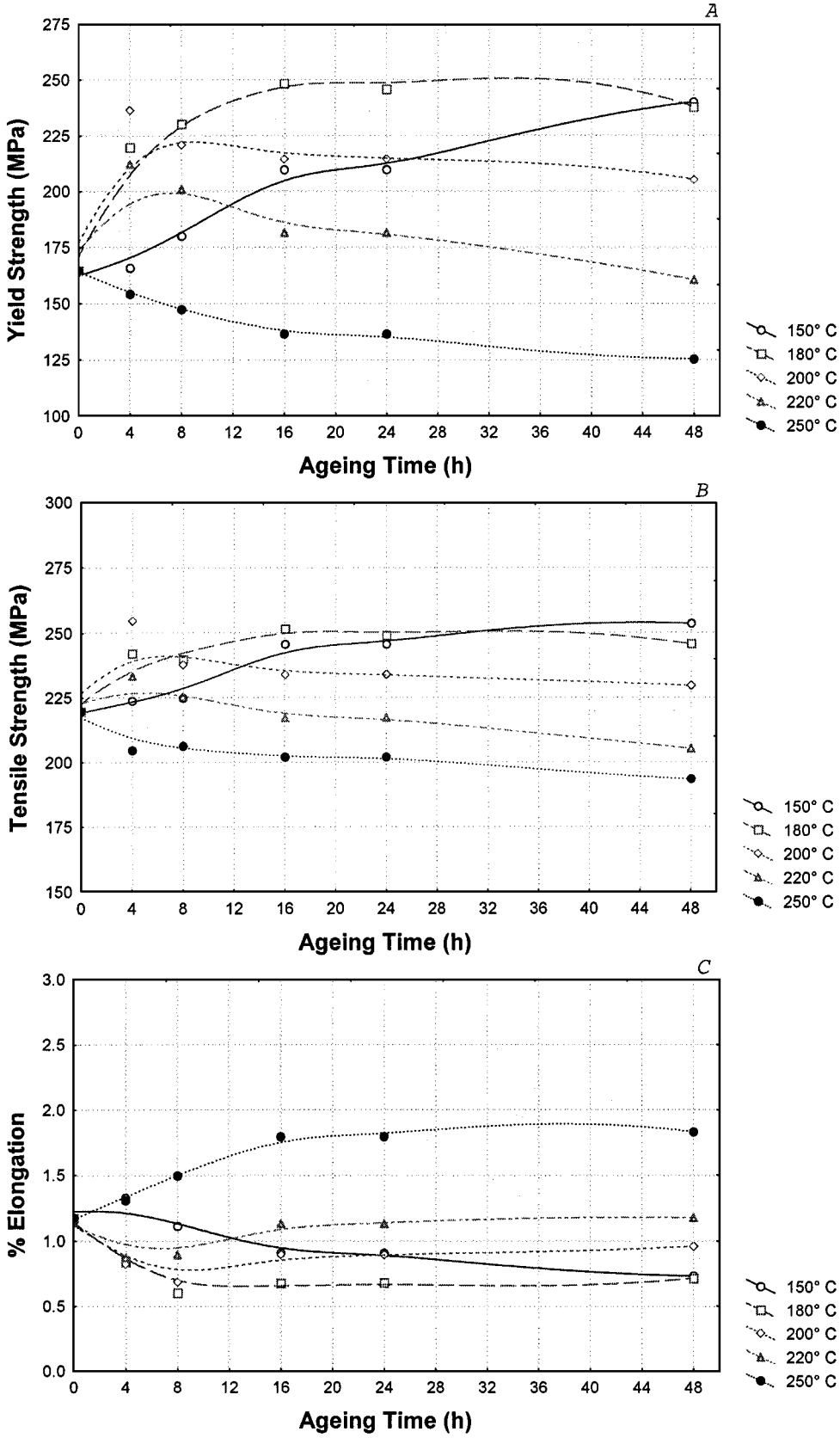

Figure 4 Variation in the tensile properties of GMST alloy in the T5 condition: (a) *YS*, (b) *UTS*, and (c) % *El*.

Grain refining of the GMS alloy (i.e., GMST alloy) resulted in increasing the as-cast elongation by approximately 0.5%, with significant changes in the alloy behaviour during ageing, Fig. 4c. This increase caused an upward shift in all plots by more or less the same value (i.e., 0.5–0.7%), depending upon the ageing temperature.

3.3. T6 treatment

3.3.1. Yield strength

After solution heat treatment (8 h at 500 °C) and quenching, the G alloy possessed a *YS* of the order of 167 MPa, Fig. 5a. Ageing at 150 °C enhanced markedly the *YS* level ∼337 MPa after 48 h. Ageing in the temperature range of 180–220 °C is characterized by the

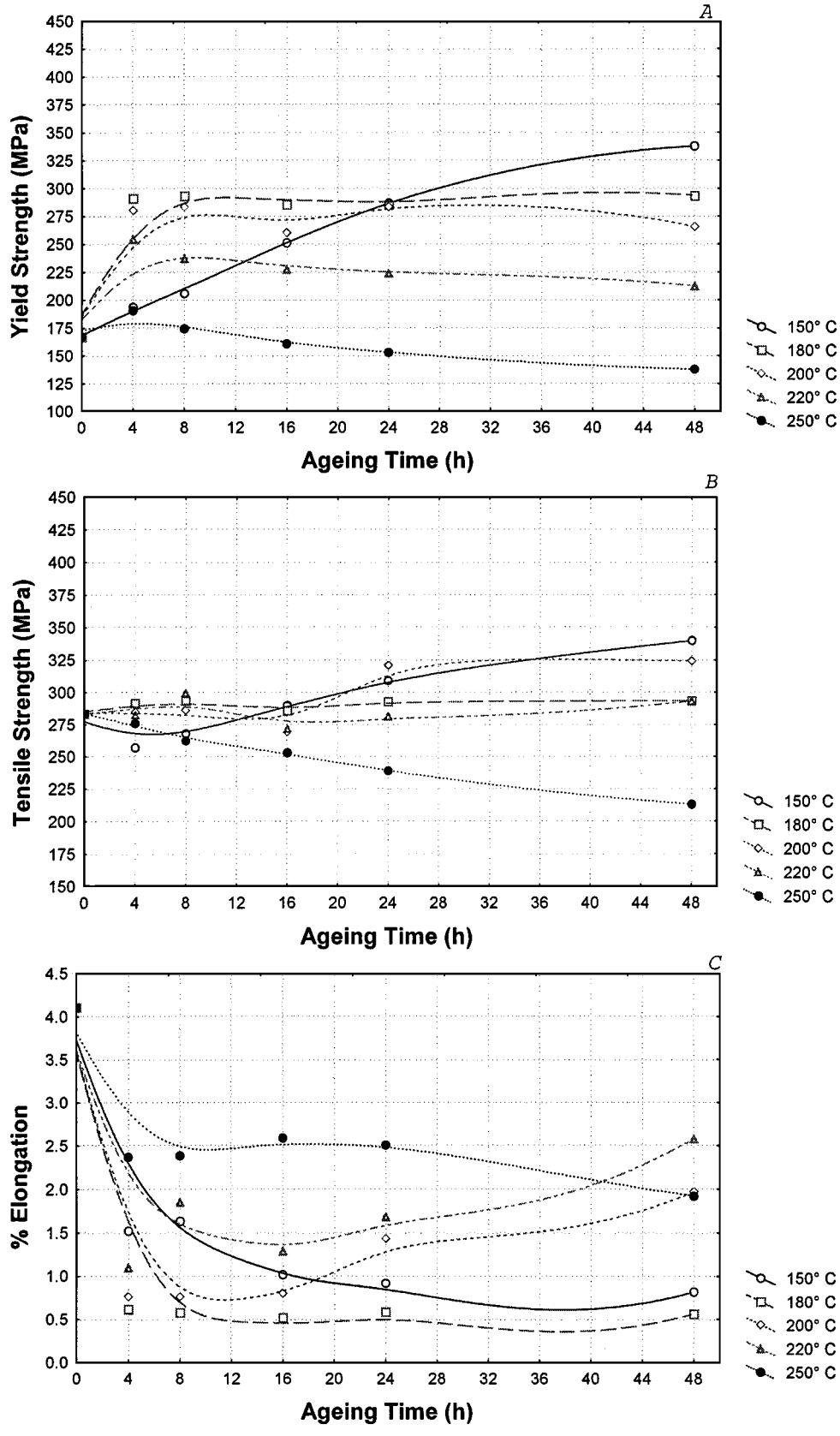

Figure 5 Variation in the tensile properties of G alloy in the T6 condition: (a) *YS*, (b) *UTS*, and (c) % *El*.

presence of peak-ageing. The maximum value, however, is reduced with the increase in the ageing temperature. Ageing at 250 °C, on the other hand, results in a linear reduction in *YS* with the ageing time. The minimum attainable value is 137 MPa, after 48 h ageing at 250 °C.

The addition of Mg increased the *YS* of the solution heat treated test bars to 213 MPa. Fig. 6a shows the excellent response of GM alloy to ageing conditions. As can be seen, each ageing temperature reveals a peak-ageing. The ageing time and maximum hardening magnitude systematically decreased with the

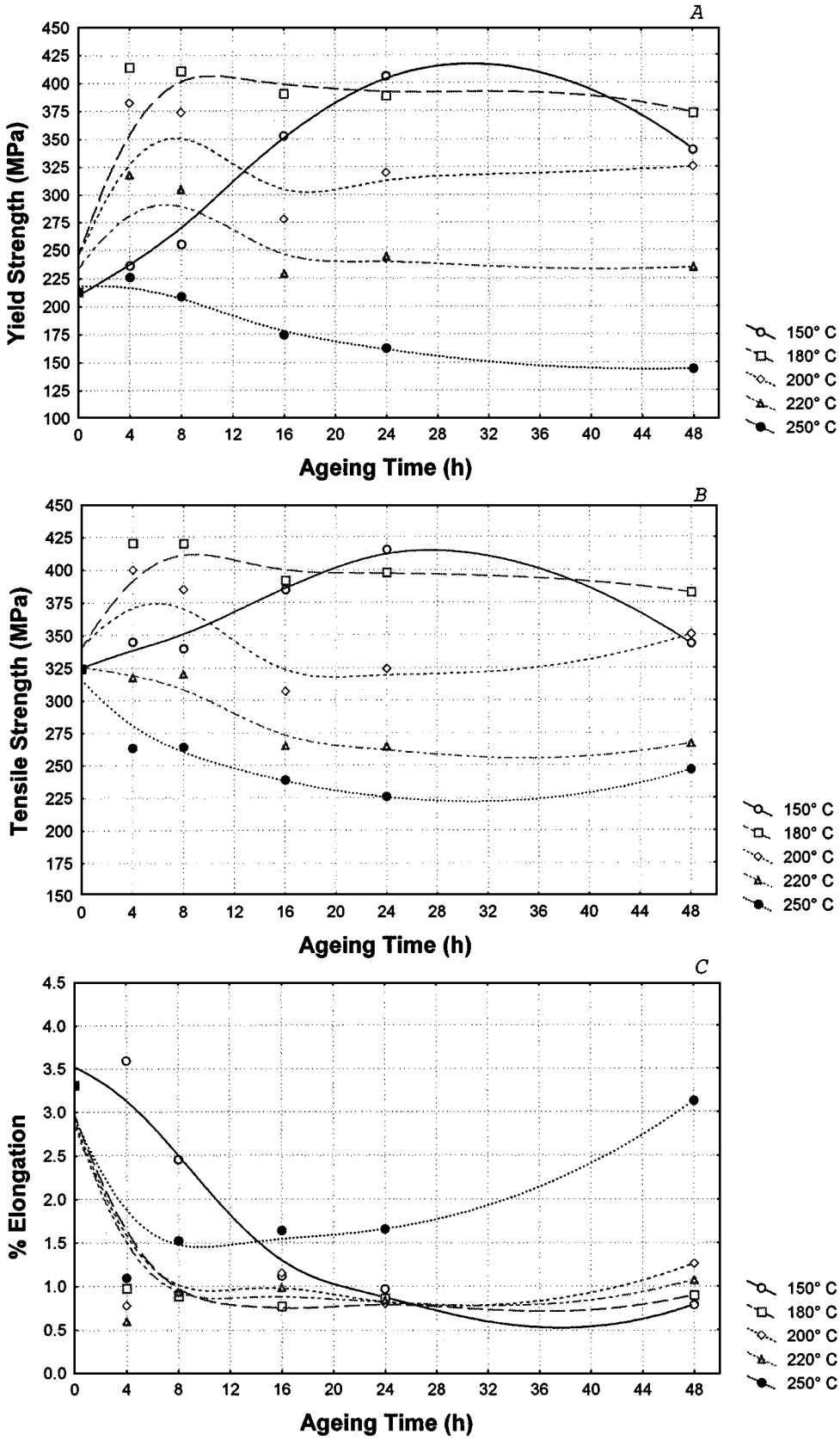

Figure 6 Variation in the tensile properties of GM alloy in the T6 condition: (a) *YS*, (b) *UTS*, and (c) % *El*.

increase in ageing temperature. The maximum *YS* value ~415 MPa was obtained when the alloy was aged either for 24 h at 150 °C or 8 h at 180 °C. A noticeable softening was observed at 250 °C.

Fig. 7a depicts the variations in *YS* values of GMS alloy upon ageing. After solutionizing, the *YS* value was about 202 MPa. This value increased by about 60%, when the alloy was aged for about 24 h at 150 °C. Ageing at temperatures inferior to 250 °C caused hardening in general, though the obtained *YS* values were naturally lower than those reported in Fig. 8a for GM alloy.

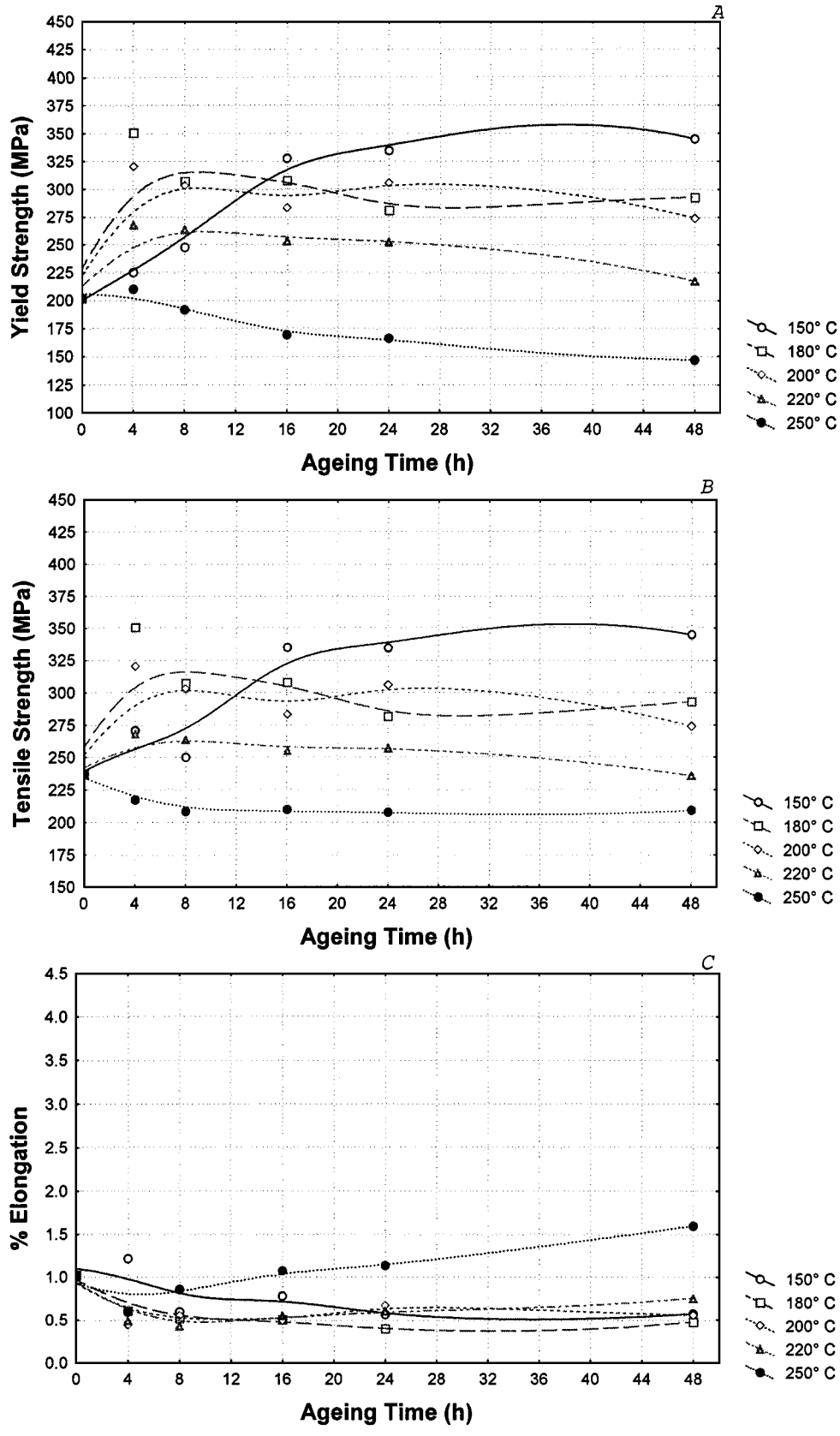

Figure 7 Variation in the tensile properties of GMS alloy in the T6 condition: (a) *YS*, (b) *UTS*, and (c) % *El*.

Although grain refining the GMS alloy (i.e., GMST alloy) did not bring about much changes in the *YS* level of solutionized test bars (206 MPa), it improved to a great extent the alloy response to ageing, as exemplified in Fig. 8a. The maximum attainable *YS* was ∼400 MPa after about 48 h at 150 °C or 8 h at 180 °C. The lowest value of *YS* was ∼37 MPa, corresponding to ageing for 24 h at 250 °C.

3.3.2. Ultimate tensile strength

The *UTS* value of solutionized test bars of G alloy is about 292 MPa. This alloy is characterized by its slow response to ageing, as shown in Fig. 5b. Ageing in the temperature range of 150–200 °C resulted in a somewhat linear hardening, with a decrease in the slope with increase in ageing temperature. The maximum reported *UTS* value was ∼340 MPa, corresponding to ageing at

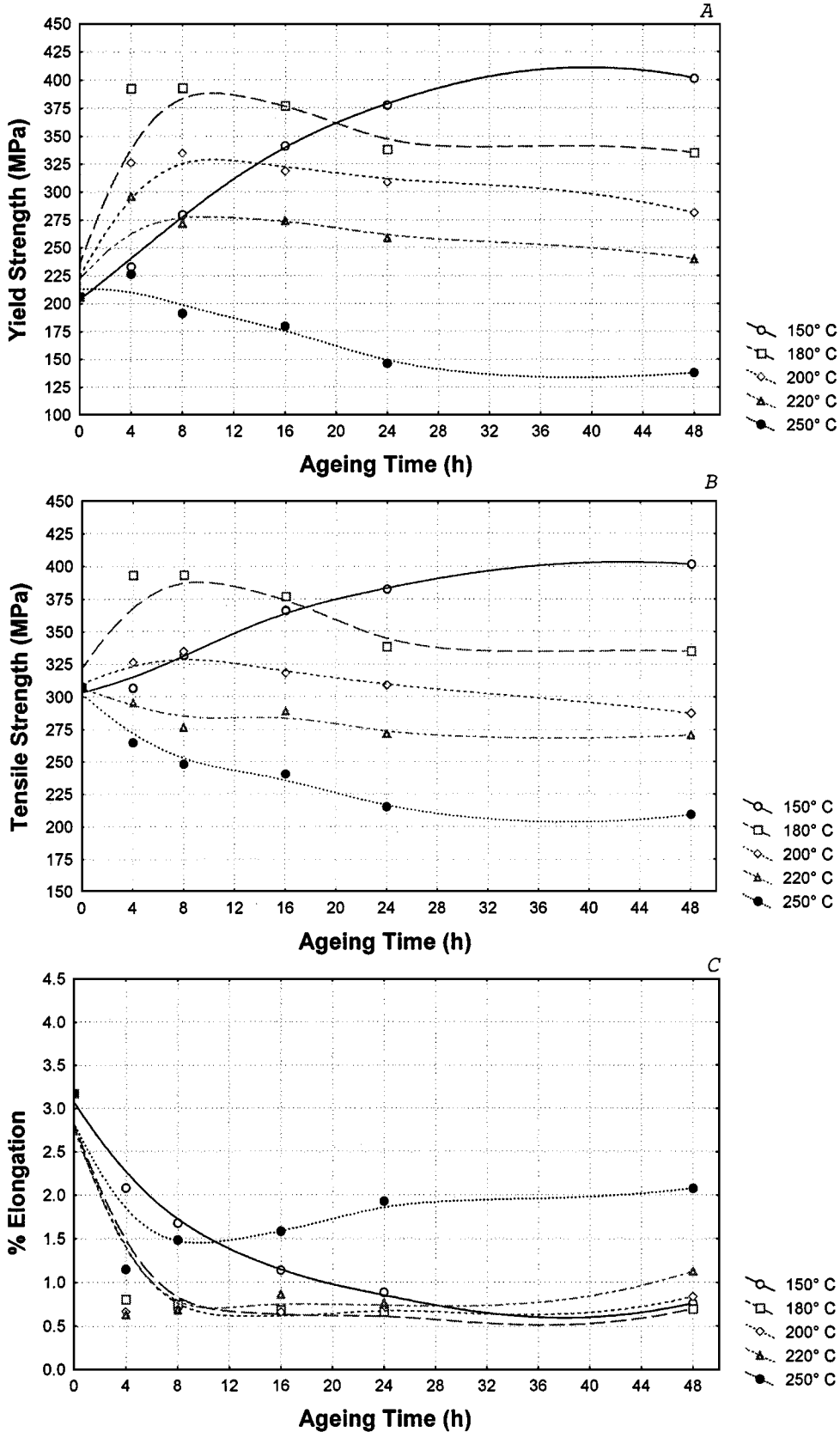

Figure 8 Variation in the tensile properties of GMST alloy in the T6 condition: (a) *YS*, (b) *UTS*, and (c) % *El*.

150 °C for 24 h. An immediate softening was observed when the alloy was aged at 250 °C.

Fig. 6b exemplifies the strong response of GM alloy to ageing conditions. The solutionized test bars revealed a value of the order of 325 MPa. Peak-ageing was clearly distinguished for ageing temperatures 150, 180, and 200 °C. Ageing at higher temperatures led to immediate softening. The maximum achievable *UTS* level was approximately 420 MPa, corresponding to either 24 h at 150 °C or 8 h at 180 °C.

As noticed earlier, the GMS alloy possessed tensile properties lower than those obtained from G alloy.

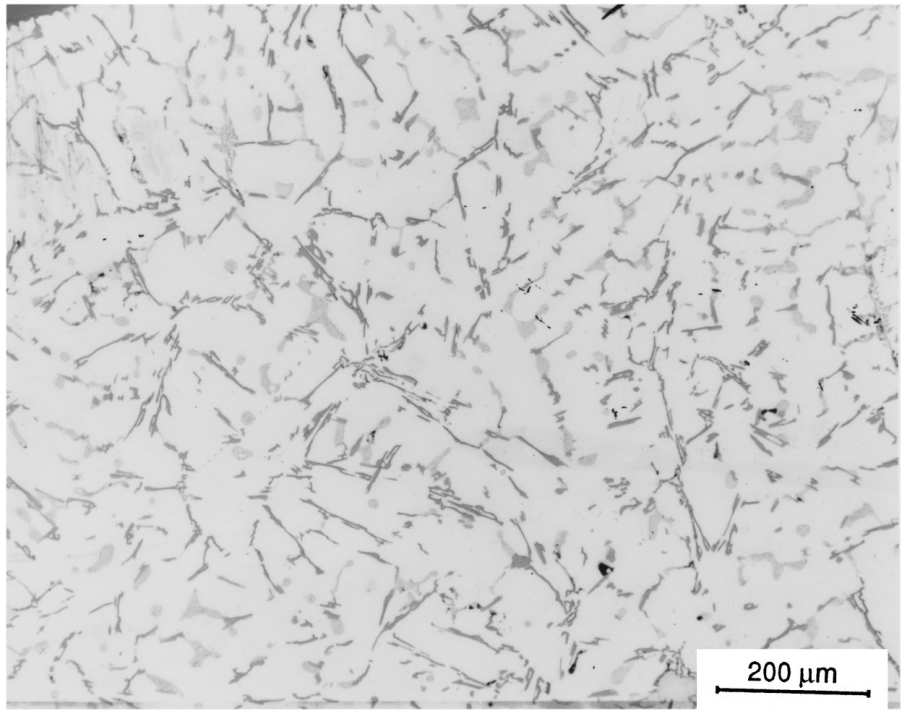

Figure 9 Microstructure of as-cast G alloy.

This observation is again reported for the variation in *UTS* values as a function of ageing conditions in Fig. 7b. The initial value of test bars prior to ageing was ∼236 MPa. This value increased substantially upon ageing at 150 °C up to 24 h (350 MPa), followed by a steady-state plateau up to 48 h. A similar ageing tendency was observed at 180 and 200 °C ageing temperatures, with not much changes at 220 °C. Ageing for 4 h at 250 °C produced the minimum *UTS* level ∼207 MPa.

Fig. 8b shows the significant improvement in hardening behaviour of grain-refined GMST alloy. The average *UTS* value of solutionized test bars was ∼307 MPa. Hardening of GMST alloy occurred upon ageing in the temperature range of 150–200 °C. The time required to reach peak-hardening decreased with the increase in ageing temperature. The maximum reported *UTS* value was about 400 MPa, obtained by ageing for times higher than 24 h at 150 °C or about 8 h at 180 °C. As observed

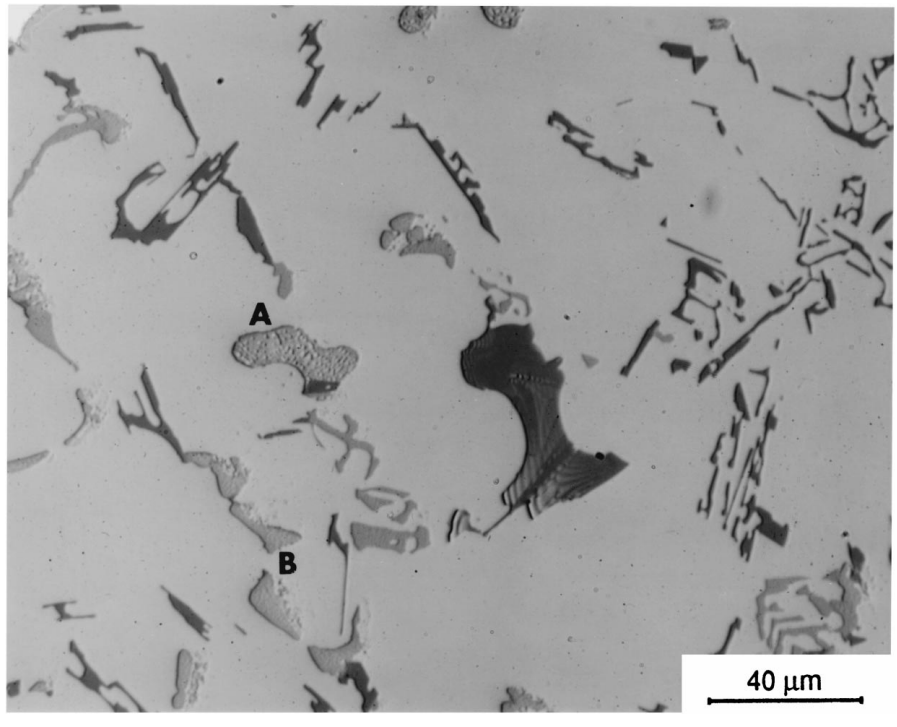

(a)

Figure 10 High magnification micrographs showing the structures of as-cast: (a) G, (b) GM, and (c) GMS alloys. (A: Al_2Cu; B: $Al_5Mg_8Si_6Cu_2$). (*Continued*).

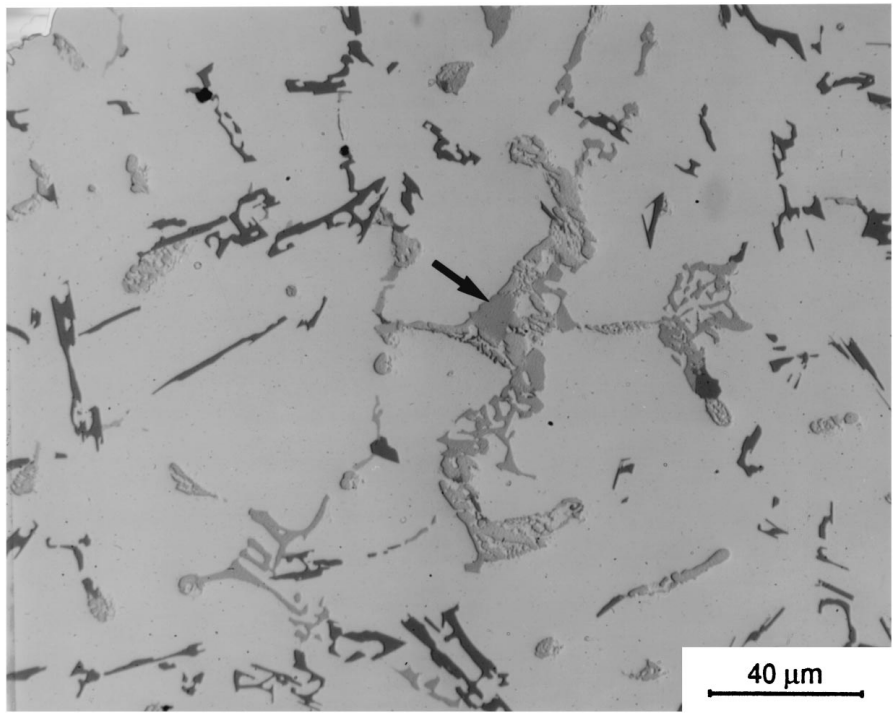

(b)

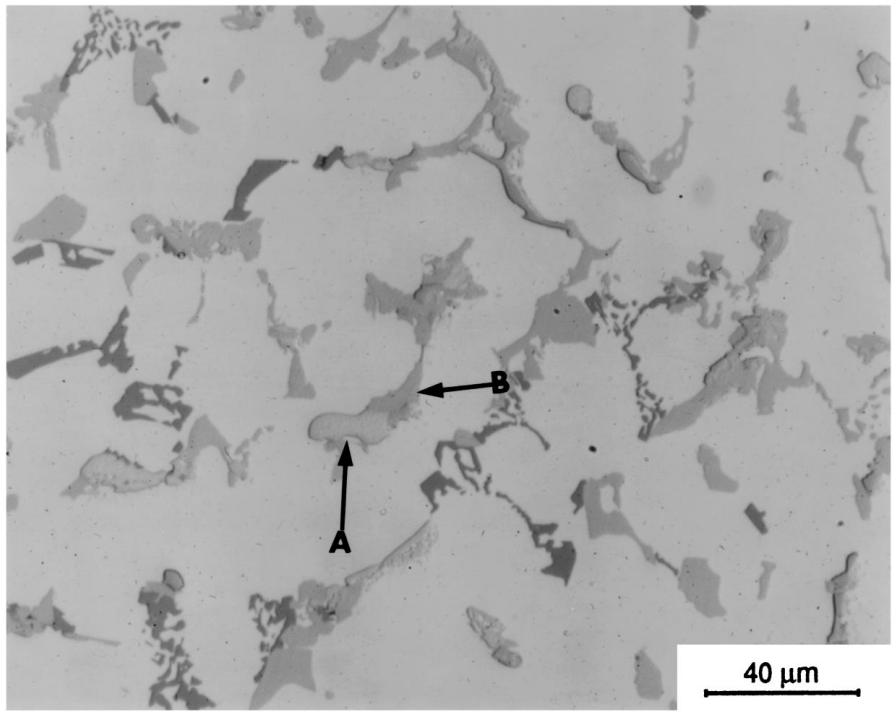

(c)

Figure 10 (*Continued*).

for GM alloy, softening commenced at 220 °C ageing temperature.

3.3.3. % Elongation

The reported % elongation of solutionized test bars of alloy G was ∼4.1%. As can be seen in Fig. 5c, ageing in the temperature range of 150–250 °C is associated with an initial decrease in the alloy ductility for ageing times up to 8 h, beyond which the ductility either remains almost constant (150–180 °C), or increases with ageing time (200–250 °C). It is interesting to note that even after ageing for 48 h at 250 °C, the attainable ductility is still inferior to that reported for the solutionized test bars (∼2.6%).

The ductility of G alloy reduced to ∼3.3% when 0.45% Mg was added. Fig. 6c shows that ageing in the temperature range of 180–200 °C produced identical values of % elongation, with a minimum value of ∼0.8% after 8 h ageing. Although ageing at 250 °C led to an initial reduction in the alloy ductility, a comparatively significant enhancement was noted when the ageing time exceeded 8 h.

The ductility of solutionized test bars of GMS alloy is fairly low ≤1%, Fig. 7c, which explains the negligible

changes in % elongation during ageing in the temperature range of 150–220 °C thereafter. A slight improvement in alloy ductility was achieved after 48 h at 250 °C ∼1.5%. On the other hand, the GMST alloy exhibited ductilities comparable to those reported for GM alloy, as exemplified in Fig. 8c.

Gauthier *et al*. [7, 8, 11] have reported the optimum solution heat treatment for G alloy (0.04% Mg) to be 8–16 h at 515 °C. This treatment is found to enhance the dissolution of Al_2Cu in the aluminium matrix (∼80%). Peak-ageing in the T6 temper is attained after 24 h at 155 °C or 5 h at 180 °C. The associated tensile properties were 253 MPa (*YS*), 295 MPa (*UTS*), and 1.2% elongation. In the over-aged condition, 24 h at 220 °C, the corresponding properties were 211 MPa (*YS*), 295 MPa (*UTS*), and 2% elongation.

The results reported in the present work on G alloy are somewhat inferior to those produced by Gauthier *et al*. e.g. 337 MPa (*YS*), 340 MPa (*UTS*), and 0.75% elongation in the T6 peak-aged condition. The difference between the two sets of results is mainly attributed to a higher solutionizing temperature applied in

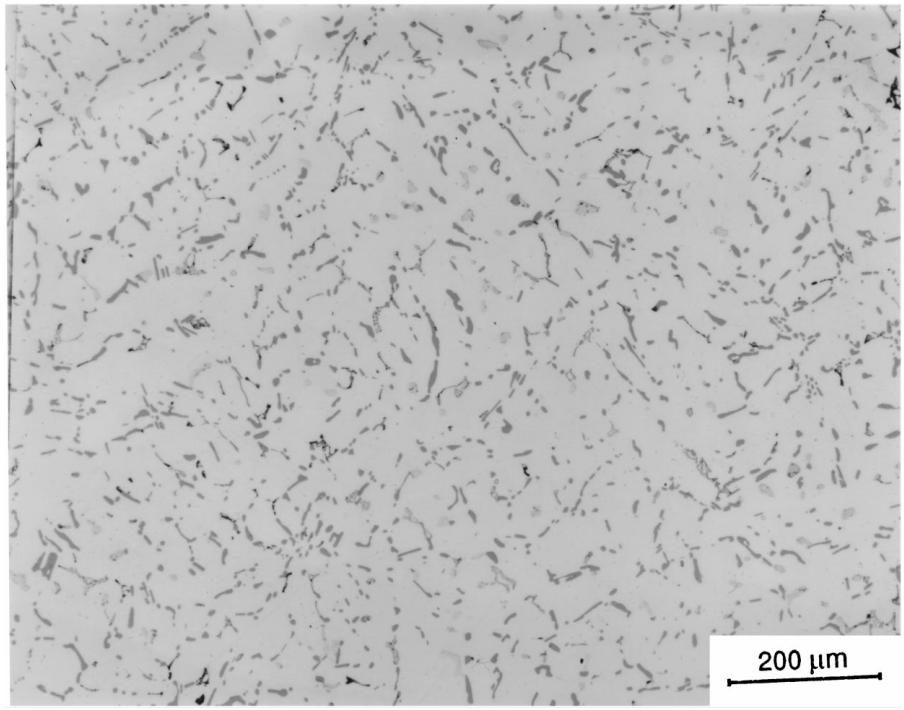

Figure 11 Persistence of α-aluminium dendritic network in GM alloy test bars solutionized at 480 °C.

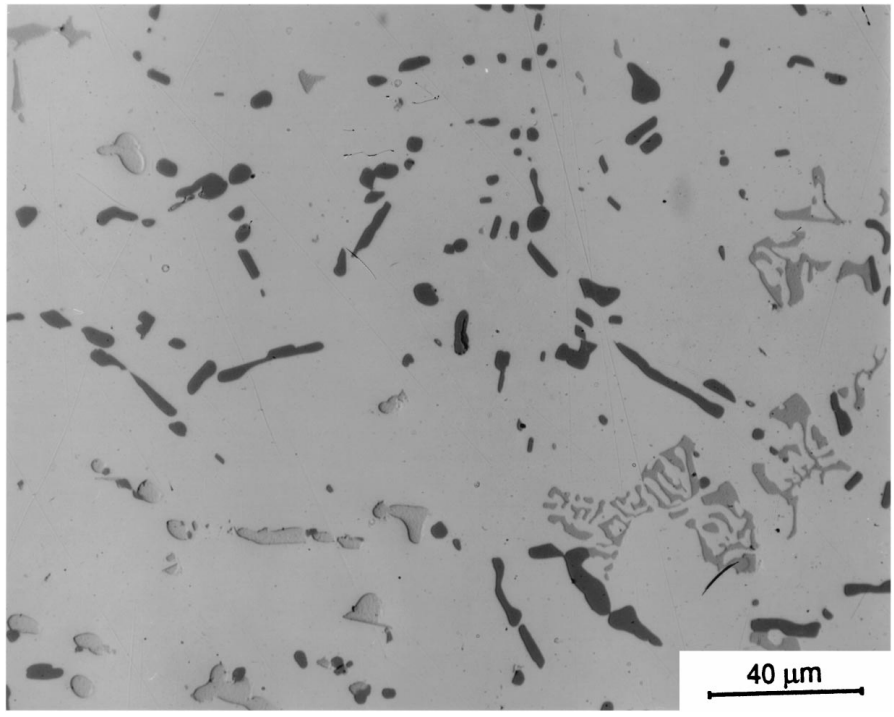

(a)

Figure 12 Microstructures of test bars solutionized at 480 °C: (a) G and (b) GM alloys. (*Continued*).

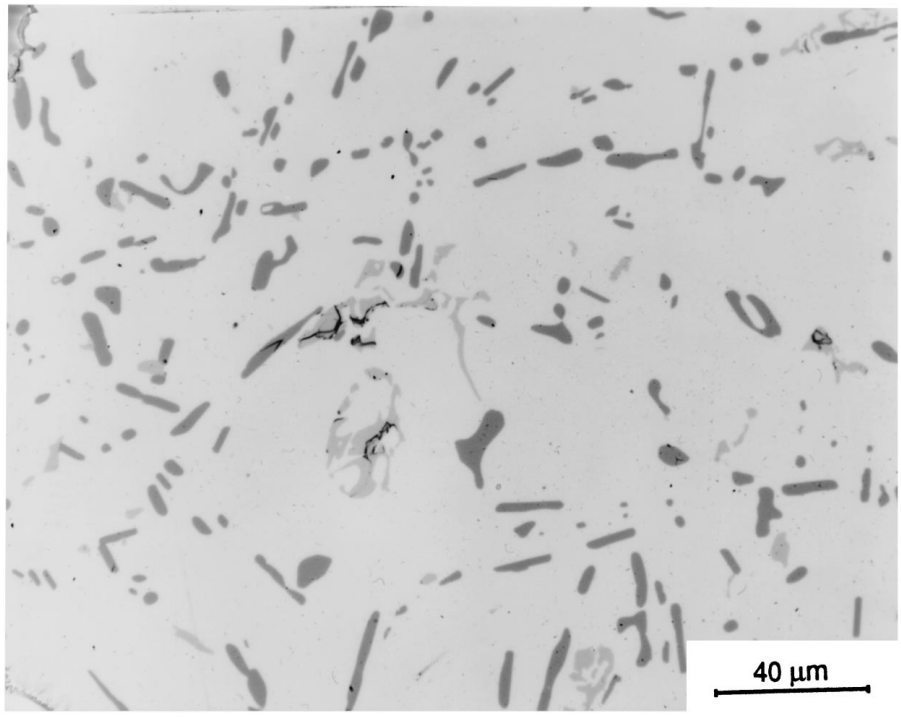

(b)

Figure 12 (*Continued*).

the former study due to the absence of the low melting $Al_5Mg_8Si_6Cu_2$ phase. Another parameter to consider is filtration of the liquid metal prior to casting. Unfiltered test bars of G alloy produced 350 MPa (*YS*), 367 MPa (*UTS*) and 0.4% elongation upon ageing for 24 h at 155 °C, following the solution heat treatment suggested by Gauthier *et al*. [11].

The effect of Mg addition on the microstructure and mechanical properties of Al-7% Si-0.3% Mg has been studied by Shivkumar *et al*. [12]. In their work, the Mg was added in amounts of 0.9, 1.8, and 2.6%. In the as-cast condition, both the base alloy and the 0.9% Mg-containing alloy showed comparable yield strengths. However, the other two alloys exhibited relatively low

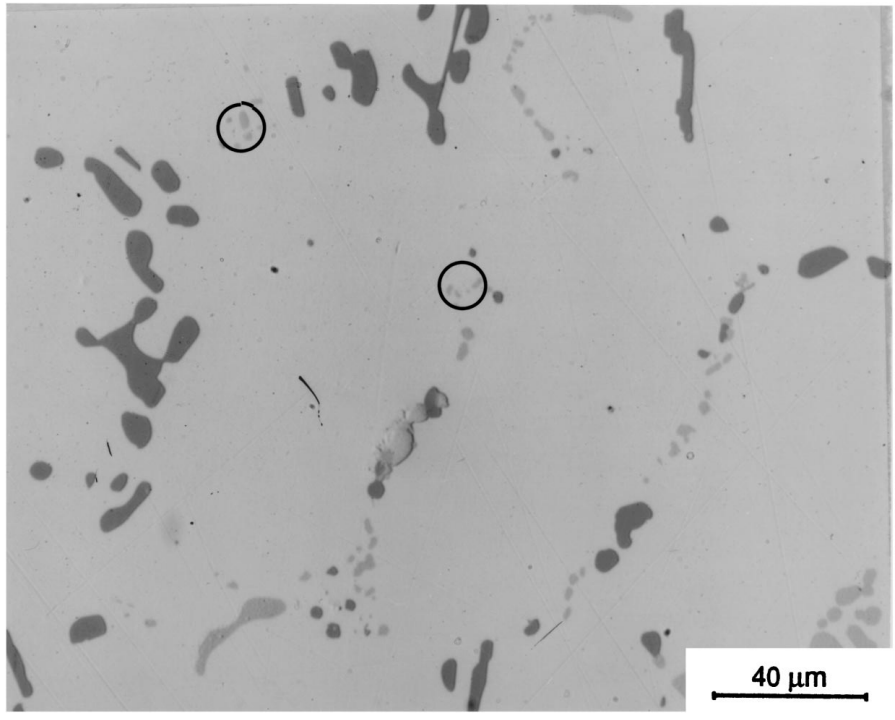

(a)

Figure 13 Dissolution of Al_2Cu and $Al_5Mg_8Si_6Cu_2$ phase particles during solutionizing at 505 °C: (a) G, (b) GM, and (c) GMS alloys. (A: Al_2Cu; B: $Al_5Mg_8Si_6Cu_2$). (*Continued*).

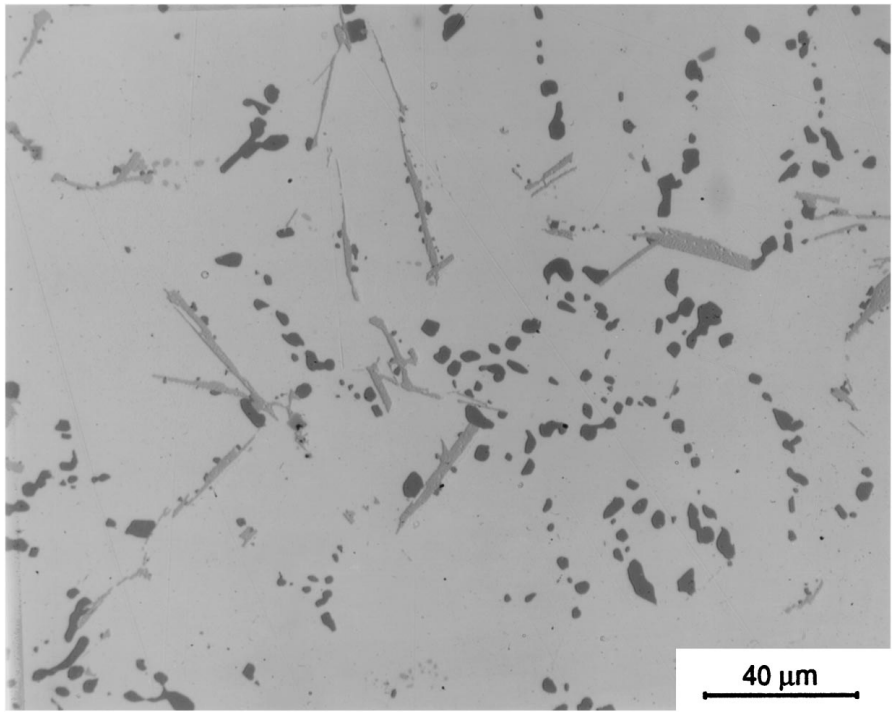

(b)

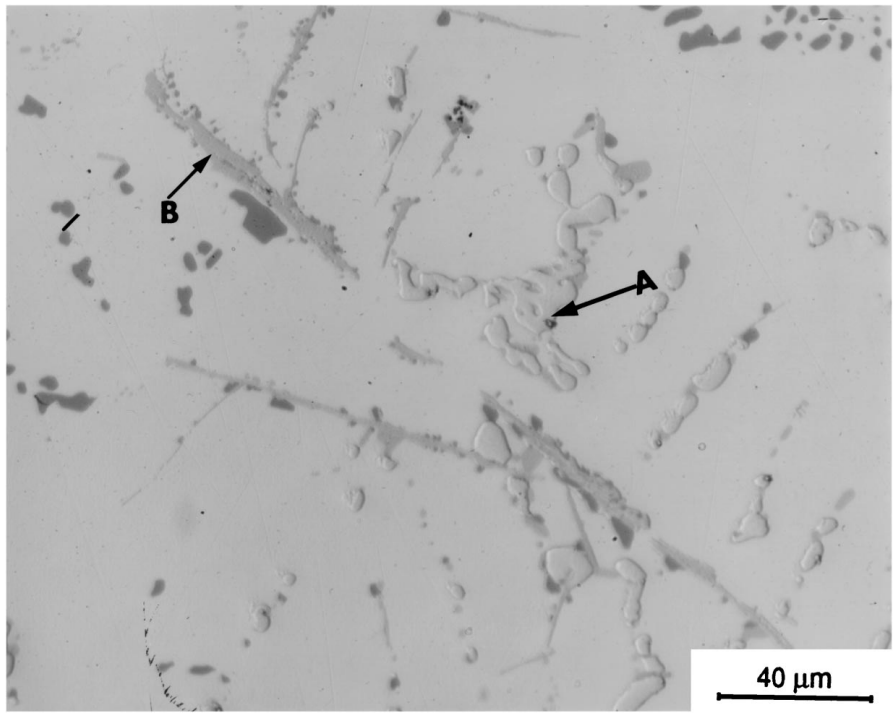

(c)

Figure 13 (*Continued*).

yield strength levels. Solution heat treatment of the four alloys resulted in almost identical *YS* values. Then, the *YS* of the 0.3 and 0.9% Mg-containing alloys increased by about 25% whereas for the other two alloys, the *YS* increased by ∼50%. In the T6 condition, maximum strength was attained after 8 h for 0.3 and 0.9% Mg-containing alloys, and after 12 h for 1.8 and 2.5% Mg-containing alloys.

In contrast to the published data [2–4], the present work shows that addition of 0.45% Mg to A319.2 alloy significantly enhances the alloy *YS* in the as-cast condition, maintaining at the same time a good level of *UTS*. Ageing the as-cast alloys for 8 h at 180 °C is sufficient to increase the *YS* and *UTS* of the GM alloy by 60 and 30%, respectively, compared to the same parameters measured for the G alloy.

It is evident from Figs 5 and 6 that Mg enhances the *YS* of solutionized A319.2 castings by at least 30%, and further by ∼40% upon ageing for 8 h at 180 °C. A similar tendency can be seen for the *UTS*. As expected, the improvement in the alloy strength is associated with a reduction in the alloy ductility.

DasGupta *et al*. [2–4] have studied the combined effect of Mg and Sr on the tensile properties of 319 alloys.

Their results show that, contrary to the negligible effect of Mg on the alloy strength, Sr in the range of 0.035–0.06% changes the morphology of the eutectic silicon from acicular to fibrous and, hence, improves significantly the alloy's mechanical properties. Beumler *et al*. [1] have analyzed the tensile properties of Sr-modified 319 alloys. Although Sr does not change the ultimate tensile strength much, it contributes markedly to the increase in the % elongation of the alloy.

In the present study, Figs 2 and 3 reveal that due to the presence of a large proportion of porosity in the modified high-Mg version of A319.2, i.e., GMS alloy, the beneficial role of Sr as a strong modification element is diminished. As a result, the GMS alloy exhibits inferior tensile properties (*YS*, *UTS*, and % *El*) compared to those obtained from unmodified GM alloy, regardless of the heat treatment condition. Similar observations have been documented by Shivkumar *et al*. [18] on the heat treatment of A356 alloys. In a recent study, Samuel *et al*. [19] have reported on the negative effect of Mg addition on the modification efficiency of Sr in 319 alloys.

The beneficial effect of grain refining in improving the strength of Al-Si-Mg castings has received considerable attention. For example, Misra and Oswalt [20] showed that grain refining A356 and A357 alloys with Ti-B influences the precipitation of Mg_2Si during

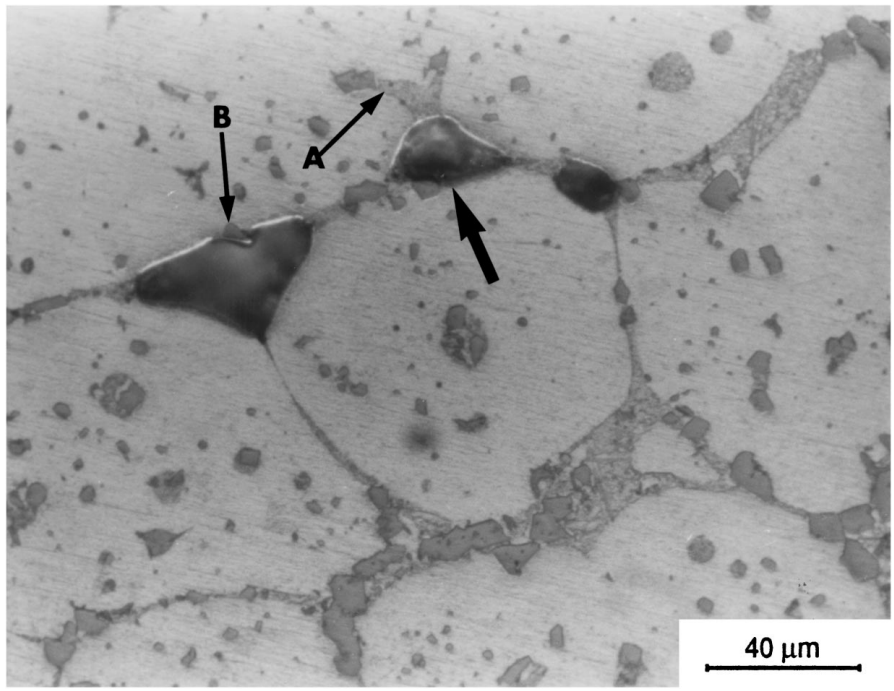

(a)

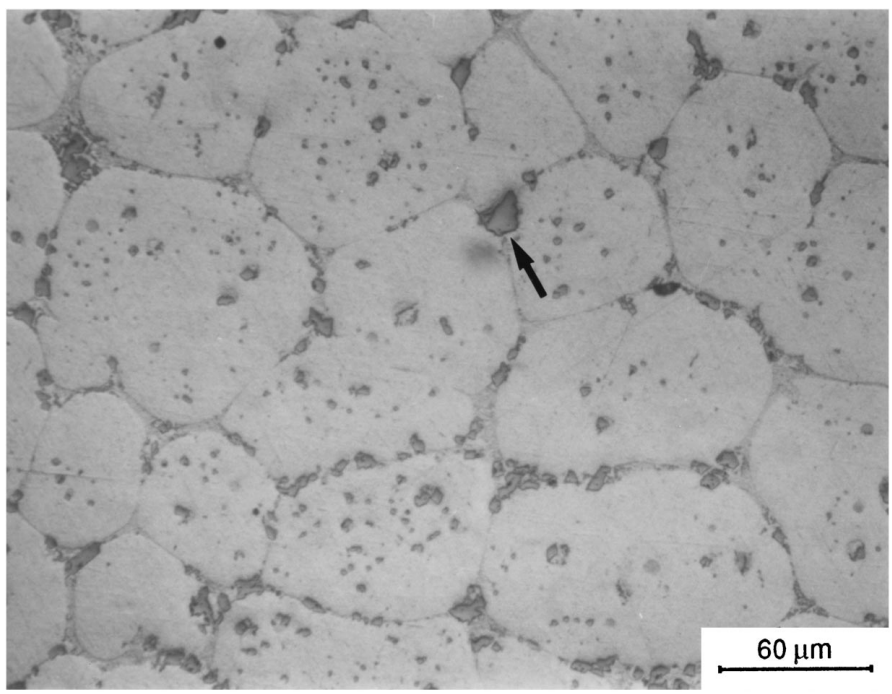

(b)

Figure 14 Incipient melting of the $Al_5Mg_8Si_6Cu_2$ phase particles in (a) GM and (b) GMS alloy test bars.

ageing, leading to the presence of a second maximum peak in % elongation which corresponds at the same time to the observed second peak-ageing. The authors attributed this particular observation to the formation of Al_3Ti particles.

It is evident from Figs 5–8 that the addition of small amounts of Al-5% Ti-1% B master alloy (measured in terms of 0.02% Ti) to Sr-modified 0.45% Mg-containing alloy (GMST alloy) would result in sounder castings with finer grain sizes. As a result, the obtained tensile properties are comparable with those obtained from the GM alloy with an appreciable consistency. It is worth mentioning here that Mg is found to possess some modification effect, especially in the absence of Sr. However, its effectiveness is much less compared to that reported for Sr [21].

It is interesting to note that ageing the GMST alloy for 8 h at 180 °C (T5 and T6 treatments) is associated with ∼30–50% and ∼10–13% increase in the *YS* and *UTS*, respectively, compared to the values obtained from G alloy treated according to the regimes listed in Table II [22].

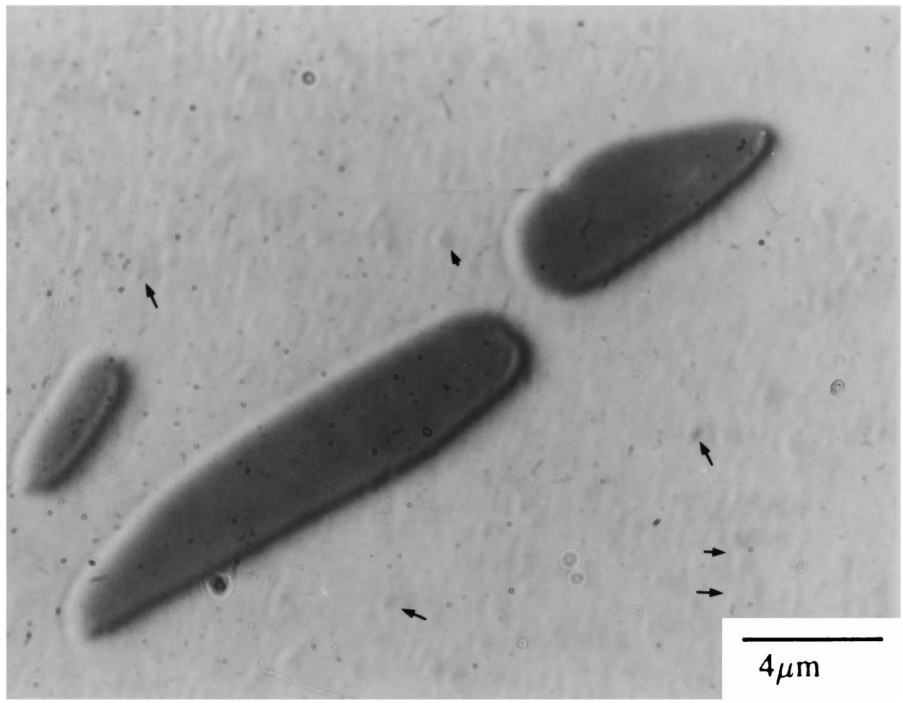

(a)

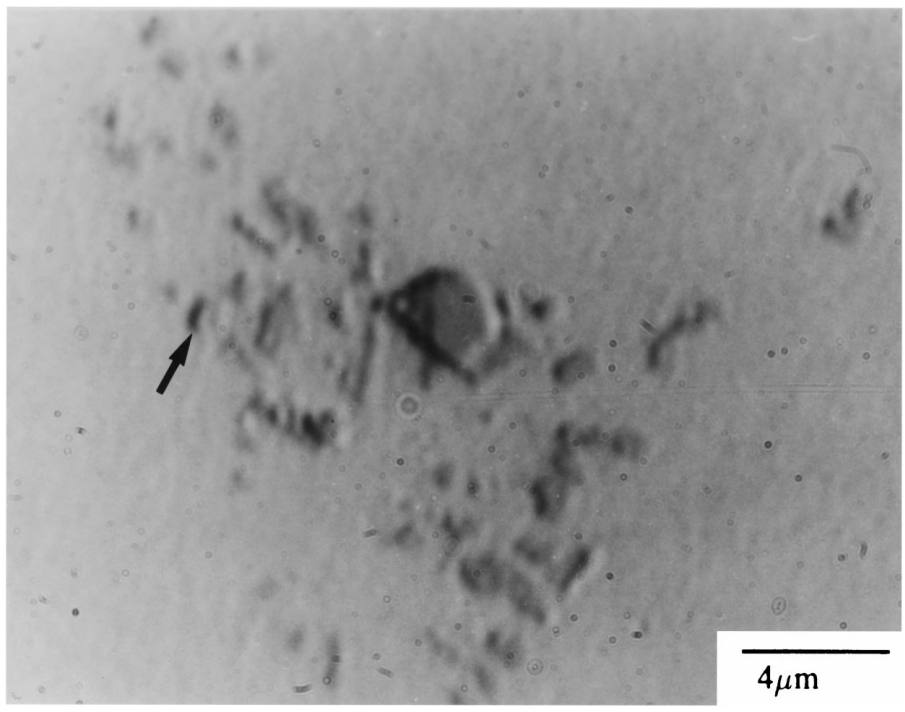

(b)

Figure 15 High magnification micrographs showing the size and distribution of Mg_2Si and Al_2Cu precipitation in GM alloy (T6 tempered) in: (a) peak-aged and (b) over-aged samples.

3.4. Microstructure

3.4.1. General features

Fig. 9 shows the as-cast structure of G alloy comprising an α-aluminium dendritic network with the eutectic silicon particles segregated into the interdendritic regions. The high magnification micrograph of G alloy, Fig. 10a, reveals that the silicon particles (or flakes) are unmodified. However, due to the relatively high cooling rate achieved by using a metallic mould ($\sim$8 °C/s corresponding to a dendritic arm spacing (DAS) of $\sim$20–25 μm), small Si particles are obtained. Two distinct morphologies of Al_2Cu phase can be seen in Fig. 10a, viz., eutectic (marked A) and block-like (marked B). Increasing the Mg content to $\sim$0.45 wt %, i.e., GM alloy, results in the formation of thick platelets of $Al_5Mg_8Si_6Cu_2$ phase (dark grey, arrowed) growing out of the Al_2Cu phase as shown in Fig. 10b. The high Mg-containing alloy appears to have a tendency to segregate the Cu phases in areas away from the eutectic silicon regions. Fig. 10c shows how modification of GM alloy with 300 ppm Sr, i.e., GMS alloy, leads to (a) modification of the eutectic silicon particles and their segregation in the form of isolated colonies, and (b) severe segregation of the Cu-phases (Al_2Cu and $Al_5Mg_8Si_6Cu_2$)

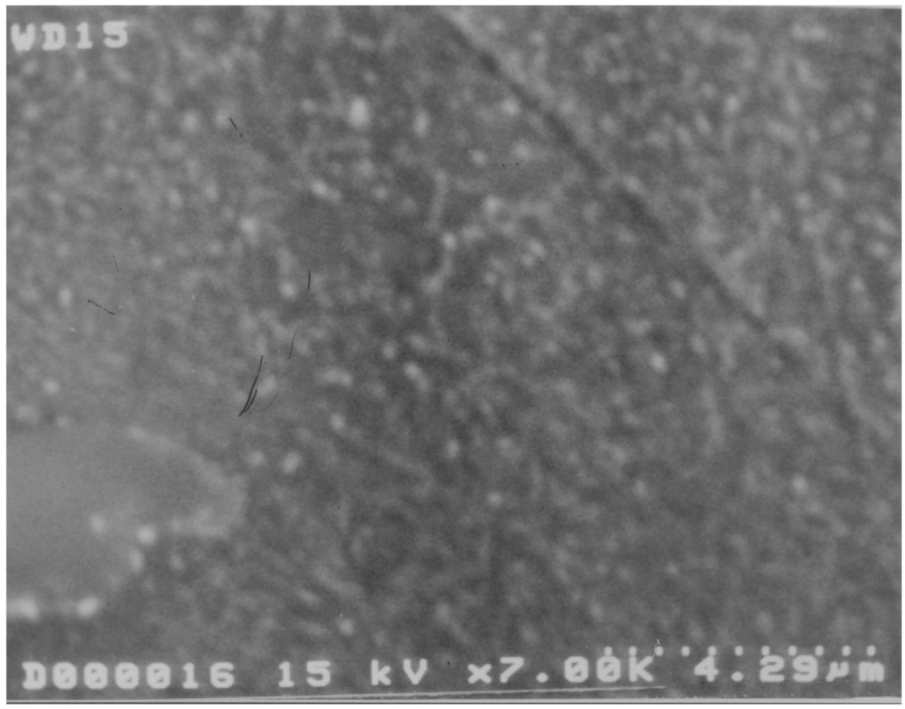

(a)

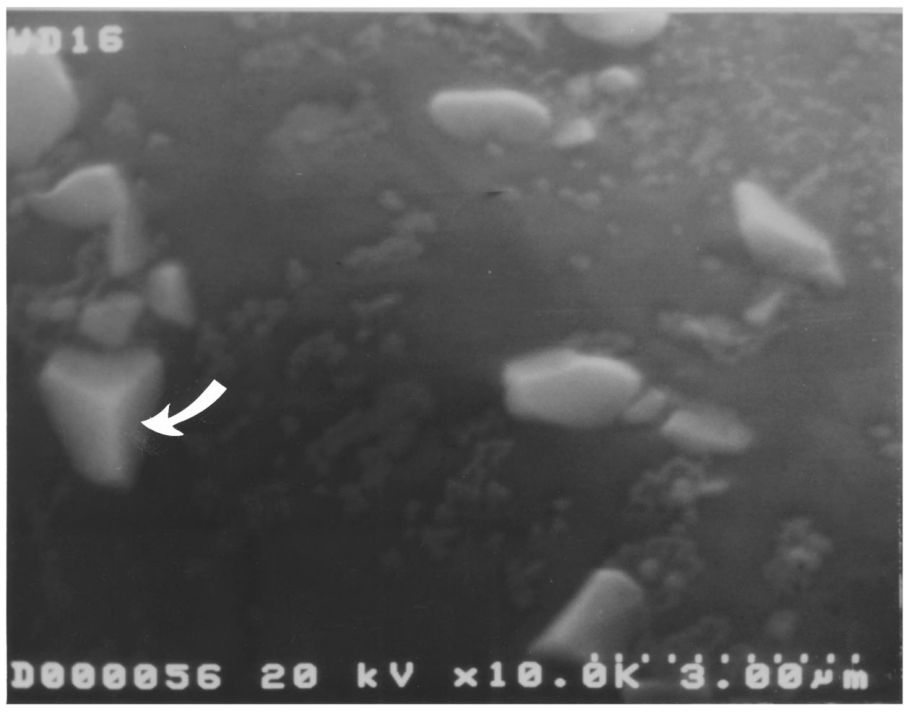

(b)

Figure 16 SEM micrographs of polished samples of GM alloy (T6 tempered) showing: (a) ultrafine particles—peak-aged condition, and (b) well defined Al_2Cu and Mg_2Si particles—over-aged condition. Arrow in (b) shows an incoherent Al_2Cu particle.

in areas away from the advancing Si colonies. As a result of such segregation, the Al_2Cu phase is mostly block-like, with a Cu concentration in the range 37–40%. This observation was confirmed by EDX analysis employing an electron microprobe analyser.

In order to obtain a maximum concentration of Mg and Si particles in solid solution, Apelian *et al*. [13] have suggested that the solution temperature should be as close as possible to the eutectic temperature. The control of temperature is very critical, because if the melting point is exceeded, there is localized melting at the grain boundaries and the mechanical properties are reduced. Temporary overheating, i.e., with respect to the melting point, is known to lead to void formation. Another phenomenon may cause microvoid formation: the soluble phases containing Mg have a tendency to leave behind microvoids when they dissolve, especially when the phase particles are large, which is the case for the GM alloy, Fig. 10. This is attributed to the density difference between the phase particles and the matrix, and the time needed for the aluminium atoms to back-diffuse into the volume formerly occupied by the

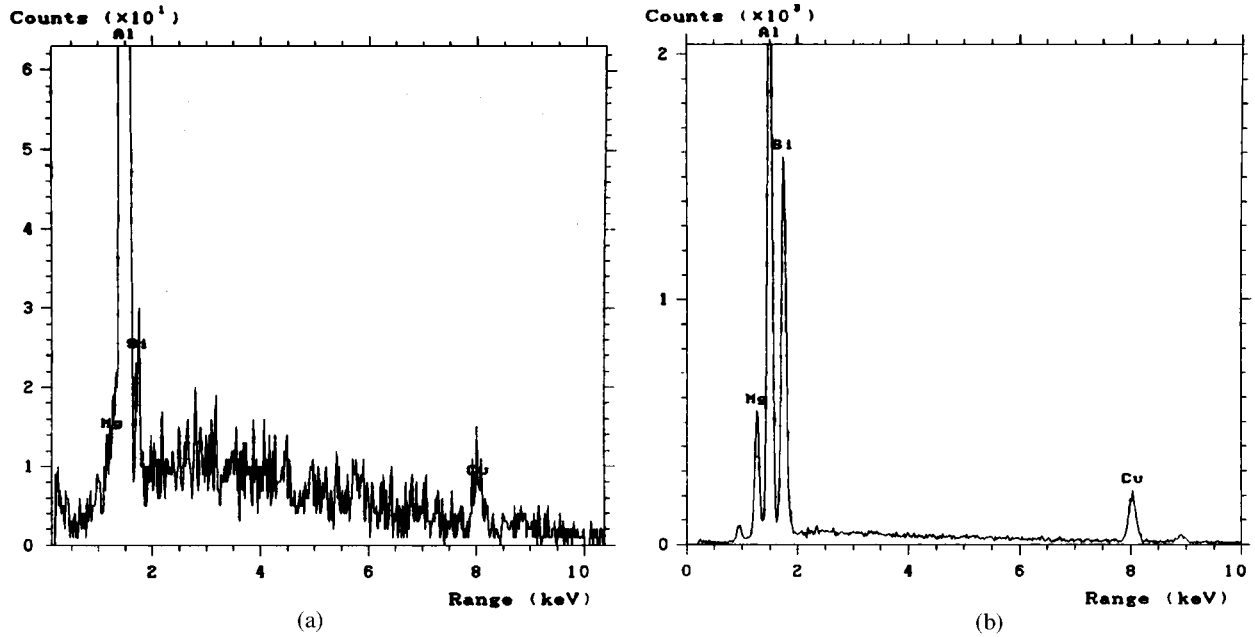

Figure 17 EDXs corresponding to precipitation shown in: (a) Fig. 16a and (b) Fig. 16b.

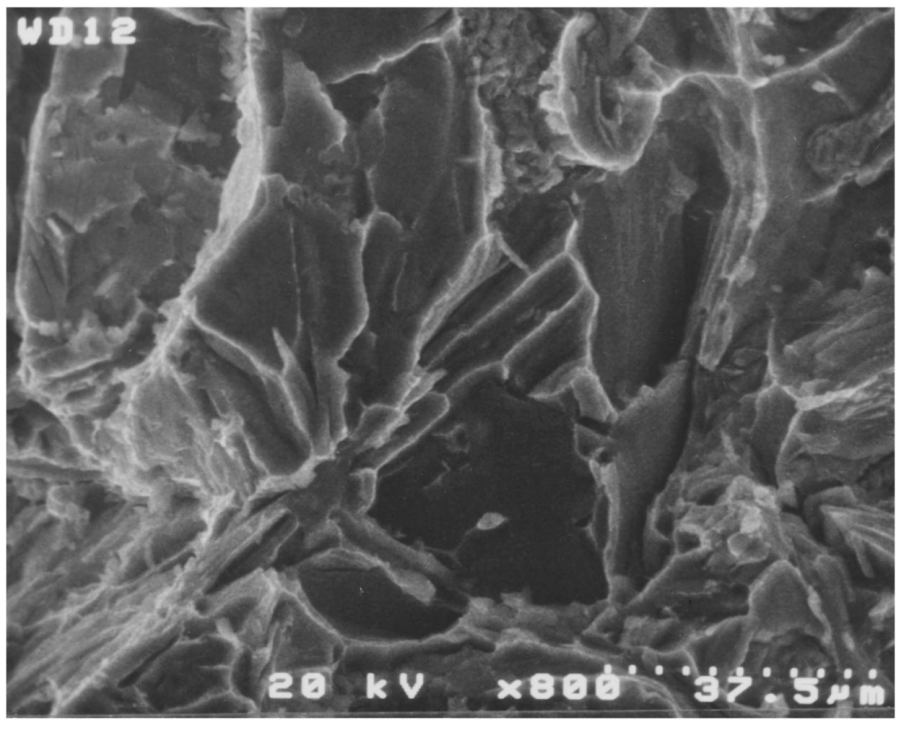

(a)

Figure 18 SEM fractographs obtained for G alloy in the (a) as-cast, (b) solution heat-treated, (c) T5-peak-aged, and (d) T6-peak-aged conditions. (*Continued*).

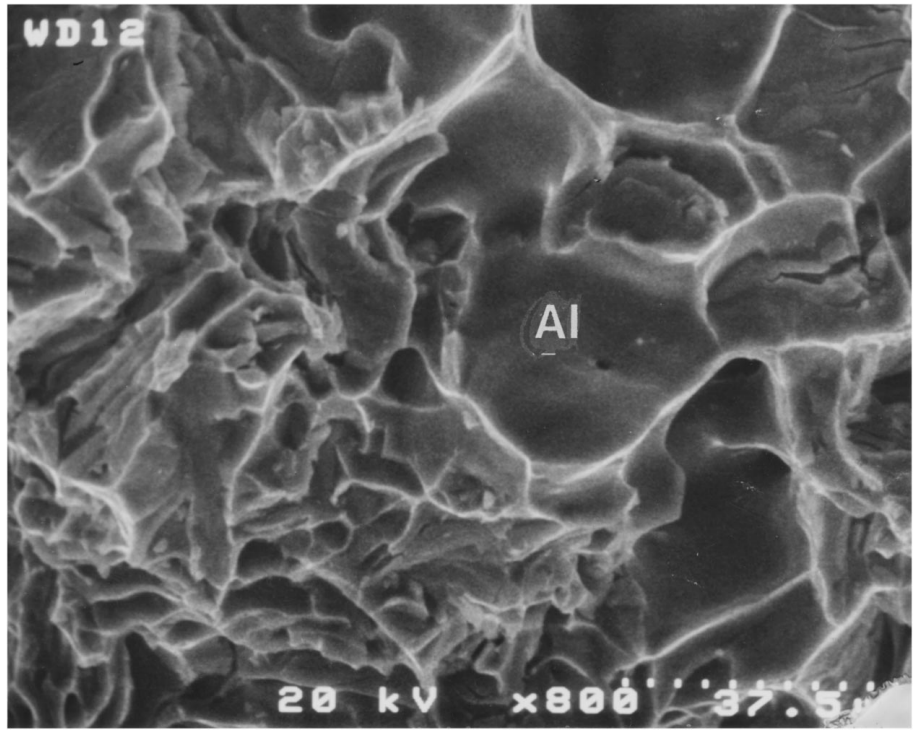

(b)

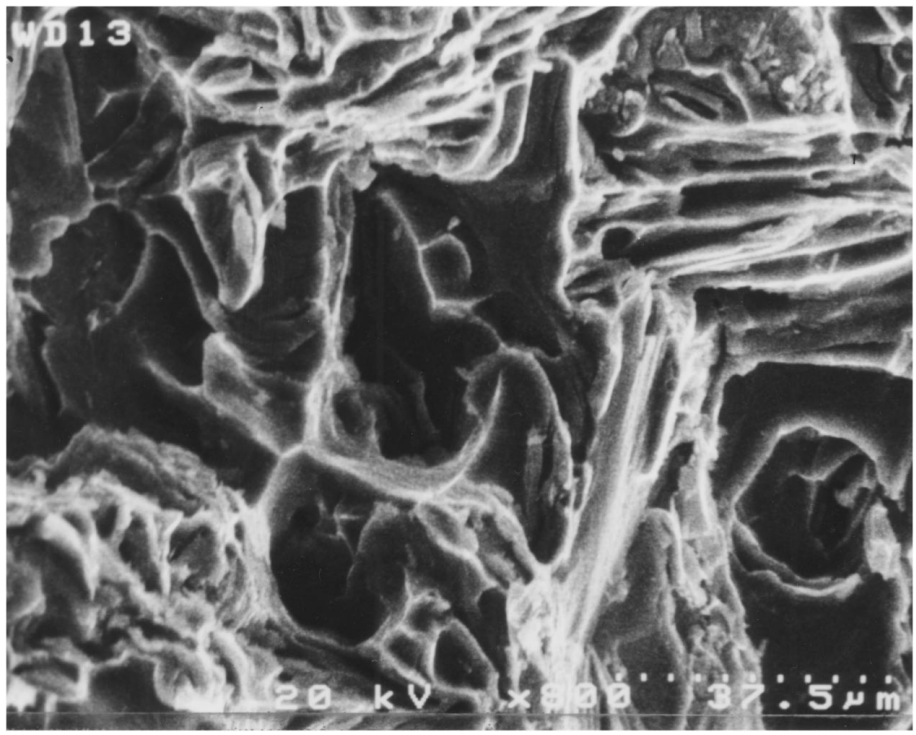

(c)

Figure 18 (*Continued*).

particles. The effect is more detrimental if these voids are combined with high temperature oxidation.

The microstructure of test bars solutionized at 480 °C (sections taken from the gauge length away from the rupture surface) reveals the persistence of the dendritic α-aluminium network, Fig. 11. A slight tendency for Si particle fragmentation is seen in Fig. 12(a) for G alloy. This tendency increases when the alloy is modified with Sr, Fig. 12(b), i.e., for GMS alloy. Dissolution of the Al_2Cu phase is evidenced when the G alloy is solutionized at 500 °C, leaving behind tiny particles (circled in Fig. 13a). Although the GM alloy exhibits a similar behaviour, dissolution of the $Al_5Mg_8Si_6Cu_2$ phase platelets is not complete, since several platelets are still seen in the microstructure, Fig. 13b. A tendency for replacing the dendritic structure by a grained one is also observed. Due to severe segregation of the Cu-containing phases in GMS alloy, dissolution of the block-like Al_2Cu phase is rather sluggish under these solutionizing conditions, i.e., 8 h at 500 °C, as shown in

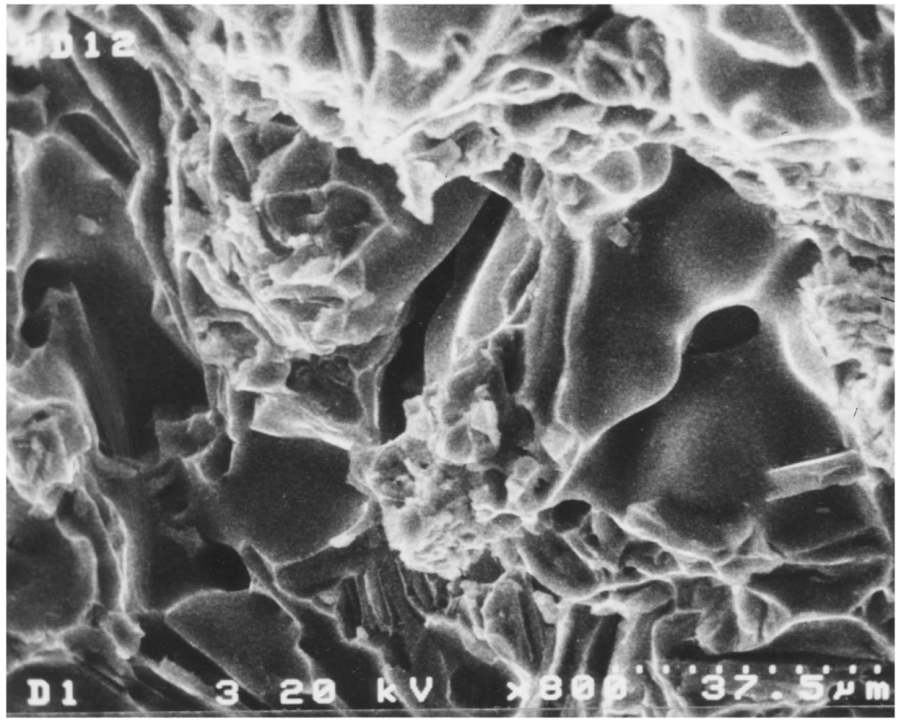

(d)

Figure 18 (*Continued*).

Fig. 13c. Thus, prolonged heating at this temperature to dissolve the $Al_5Mg_8Si_6Cu_2$ and Al_2Cu phase particles may be suggested.

As discussed earlier, the first drop of liquid metal forms when the GM alloy is heated at temperatures close to or higher than 505 °C. Solutionizing at 505 °C is characterized by the replacement of the α-aluminium dendritic network by an equiaxed structure, Fig. 14a. Both the Si and Cu-phase particles are segregated into the grain boundaries. In Fig. 14a, the remaining unmelted phase can still be seen (arrowed-A), with Si particles observed at the edges of the melted

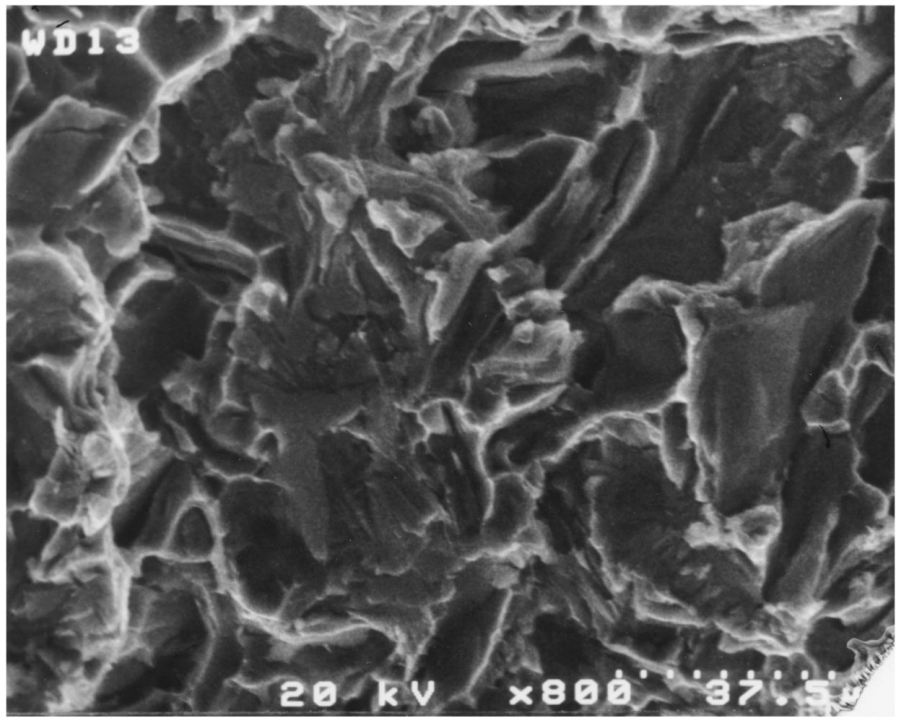

(a)

Figure 19 SEM fractographs obtained for GM alloy in the (a) as-cast, (b) solution heat-treated, (c) T5-peak-aged, and (d) T6-peak-aged conditions. (*Continued*).

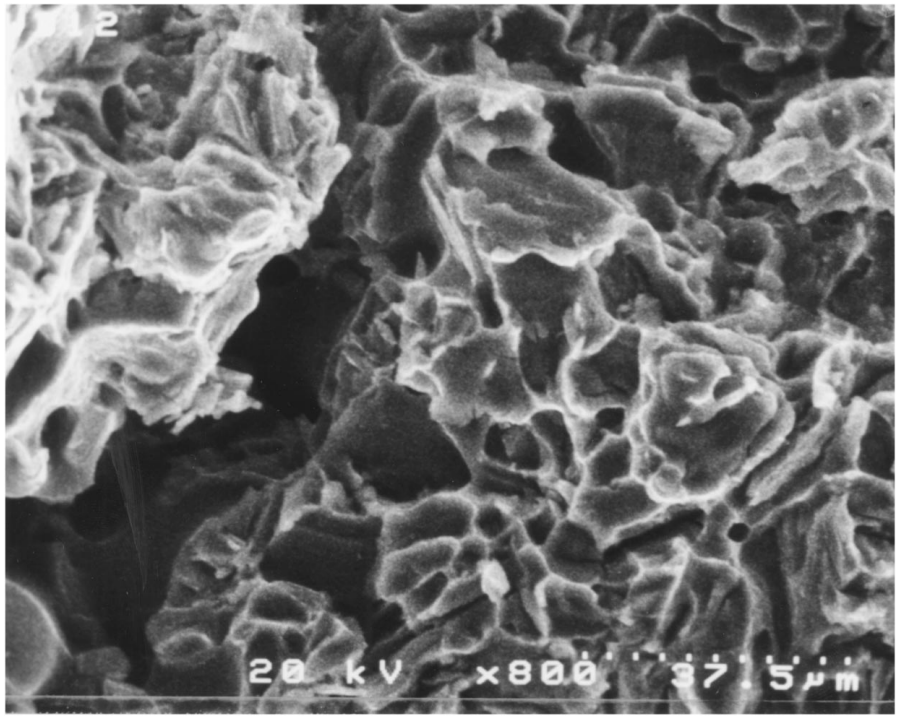

(b)

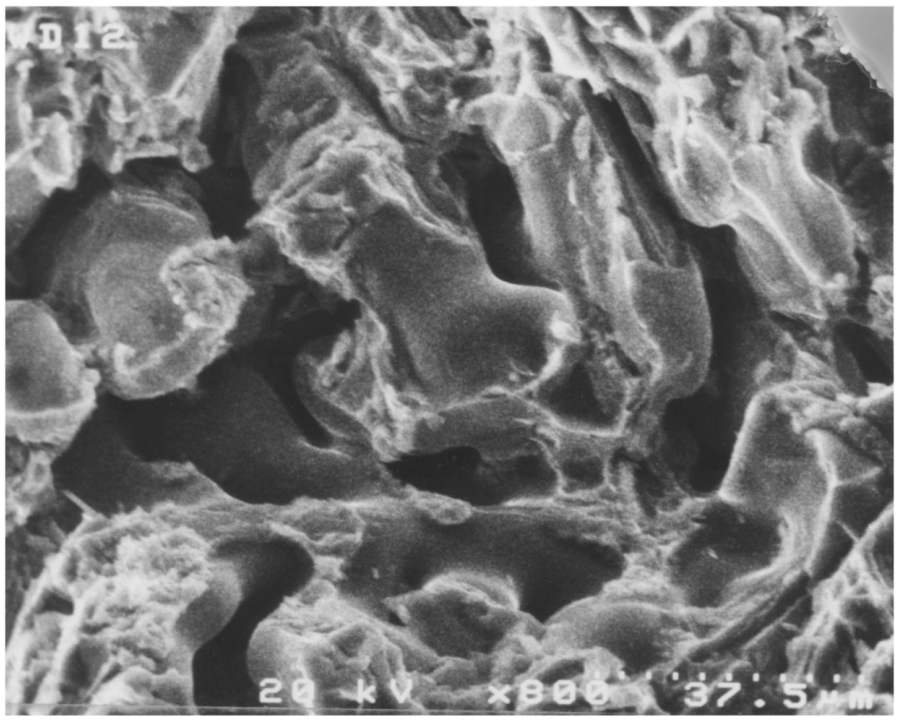

(c)

Figure 19 (*Continued*).

particles (arrowed-B). Modification of the GM alloy with 300 ppm Sr has no effect on the incipient melting of the $Al_5Mg_8Si_6Cu_2$ phase particles, as is evident in Fig. 14b. The arrow in the figure indicates the molten particles at the grain boundaries. Narayanan *et al*. [23] have reported on the incipient melting of the copper phases in 319 alloy containing 0.3 wt % Mg when the alloy was treated in the non-equilibrium condition, i.e., above 480 °C. In this case, melting initially took place at grain boundaries and in the interdendritic regions, leading to the formation of spherical liquid droplets. On quenching this liquid, re-precipitation of silicon and other intermetallics occured.

Dissolution and melting of Al_2Cu phase in A319.2 aluminium alloy has been studied in detail by Samuel *et al*. [24]. Dissolution of the eutectic ($Al + Al_2Cu$) phase takes place at temperatures close to the final solidification temperature of the alloy ∼480 °C, the dissolution kinetics accelerating with increasing solution temperature ∼515 °C. Dissolution of the phase occurs through its fragmentation into smaller segments that gradually dissolve into the surrounding Al matrix with

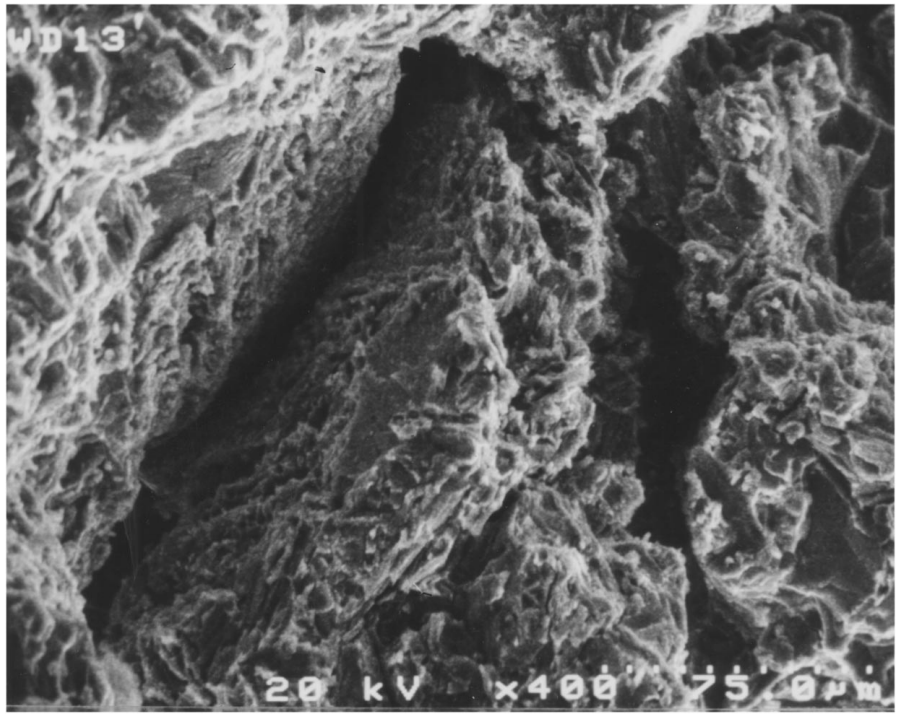

(d)

Figure 19 (*Continued*).

an increase in solution treatment time. At higher solution temperatures, e.g., 515 °C, melting of the eutectic copper phase occurs, the molten particles transforming into a shiny structureless phase upon quenching.

3.4.2. Phase precipitation

Fig. 15a and b compare, respectively, the size and distribution of the precipitated phase particles when GM alloy test bars were treated in the peak-aged (16 h at 150 °C) and over-aged (48 h at 250 °C)—T6 conditions. As mentioned earlier, hardening occurs by cooperative precipitation of Al_2Cu and Mg_2Si phase particles. In the peak-aged condition, the Al_2Cu and β' Mg_2Si are metastable phases, coherent with the matrix. Increasing the ageing time or ageing temperature increases the size of these particles, with gradual change in their chemical composition. As a result, equilibrium $\theta(Al_2Cu)$ and $\beta'(Mg_2Si)$ phases in the form of incoherent particles are responsible for the observed drop in the alloy strength. The precipitated particles in the peak-aged condition are extremely fine to be clearly examined by optical microscopy, as is evident from Fig. 15a. In fact, these particles appear in the form of pinpoints (arrowed). In the over-aged condition, Fig. 15b, the particles are visible and can be distinguished from the other dissolved phases (see arrow in Fig. 15b). In order to arrive at a clear understanding of the nature of these phases, the polished samples were deeply etched using Keller's solution and examined by scanning electron microscopy (SEM) equipped with an energy dispersive X-ray (EDX) system.

Fig. 16a shows the homogeneous distribution of the precipitated particles throughout the matrix, when the test bars were in the peak-aged condition. The size of these particles varies between 0.2 and 0.5 μm. No definite particle boundaries can be seen. The associated EDX spectrum (Fig. 17a) reveals very diffused Mg and Cu reflections, indicating the coherency of the particles with the matrix.

In the over-aged condition, Fig. 16b, two types of phases could be distinguished viz., Al_2Cu and Mg_2Si. The Al_2Cu phase particles are characterized by their large sizes and defined boundaries indicating their incoherency with the matrix (arrowed). The associated EDX spectrum, Fig. 17b, reveals strong Mg and Cu reflections compared to those shown in Fig. 17a for the peak-aged samples.

3.5. Fracture behaviour

The fracture surface of the as-cast samples revealed, in general, a ductile rupture mode. Fig. 18a is a high magnification fractograph exemplifying the brittle nature of unmodified eutectic silicon particles in such samples. Solution heat treatment for 8 h at 500 °C resulted in partial spheroidization of the Si particles, as shown in Fig. 12. This process is associated with a noticeable enhancement in the alloy ductility. As can be seen from Fig. 18b, a large number of small dimples is replacing the area that was occupied by the unmodified Si flakes. When the casting is solutionized at 500 °C for 8 h, the microstructure is characterized by (a) partial spheroidization of the eutectic Si particles and a greater surface area of ductile aluminium matrix, (b) dissolution of a large proportion of Mg and Cu, and (c) a homogenized distribution of alloying elements.

Ageing the as-cast test bars for 4 h at 180 °C (T5, under-aged condition) does not introduce noticeable changes in the general rupture features. However,

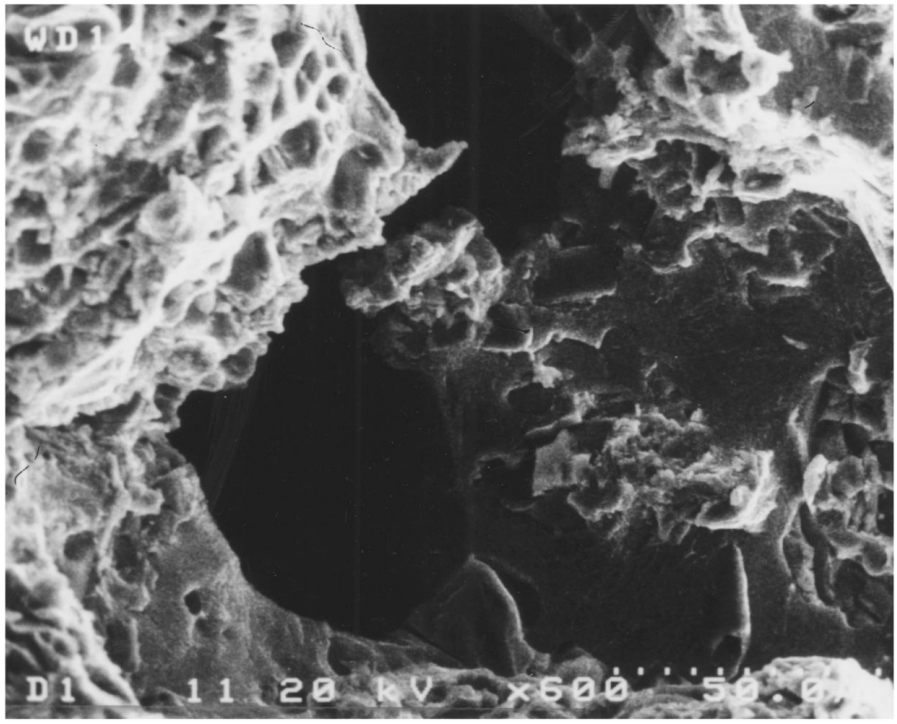

(a)

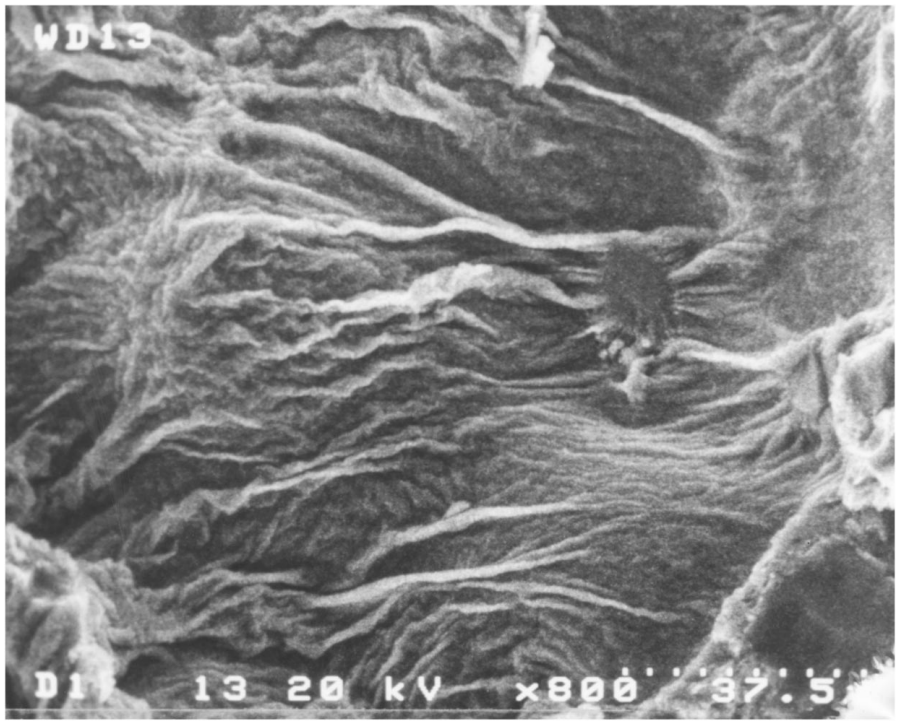

(b)

Figure 20 Incipient melting of Cu-containing phases in GM alloy solutionized at 540 °C for 8 h, showing: (a) large pores and (b) brittle rupture of solidified particles.

several microcracks (secondary cracks) are seen passing through the Si, Fe and Cu-containing phase particles in the interdendritic regions, which is in good agreement with observations reported earlier [11]. Increasing the ageing time at 180 °C to 16 h (corresponding to the peak-aged condition) leads to more precipitation of the hardening phases which causes alloy embrittlement, as evident from the greater number of secondary cracks observed in Fig. 18c.

Subsequent ageing of the solutionized test bars for 8 h at 150 °C (T6, under-aged condition) allows for a better control of the decomposition of the supersaturated matrix and, hence, the precipitation rates of Al_2Cu and Mg_2Si phase particles. Fig. 18d exhibits rather brittle cleavage fracture of most of the intermetallic phase particles. Also, relatively deep microcracks propagating into the matrix beneath the fracture surface can be seen. As expected, increasing the ageing time, i.e., 16 h

(corresponding to the peak-aged condition), contributes to the alloy brittleness and, therefore, more secondary cracks.

Increasing the Mg concentration to 0.45% results in partial modification of the eutectic Si particles [24]. Fig. 19a shows smaller Si particles and less cleavage rupture compared to that observed for G alloy in the as-cast condition. However, Mg addition increases the volume fraction of Cu-containing intermetallics. Solution heat treatment of GM alloy at 150 °C for 8 h seems to be more effective with respect to the spheroidization of the eutectic Si particles which, in turn, enhances the alloy ductility as evidenced by the dimple structure shown in Fig. 19b.

The increase in the concentration of Mg is expected to cause precipitation of a relatively large volume fraction of Mg_2Si when the as-cast test bars are aged for 4 h at 180 °C. In the peak-aged condition, i.e., 16 h at 180 °C, the alloy reaches its minimum value of % elongation, resulting in severe secondary crack formation throughout the matrix, Fig. 19c. As mentioned earlier, a T6 treatment accelerates the precipitation of ultra-fine Al_2Cu and Mg_2Si phase particles which render the alloy its strength. The fracture surface of peak-aged test-bars (16 h at 150 °C) is shown in Fig. 19d. The cracks are mainly localized in the interdendritic regions.

As shown in Fig. 14, solution heat treatment of the GM alloy at temperatures much higher than the fusion point of Al_2Cu and $Al_5Mg_8Si_6Cu_2$ phases causes partial or complete melting of these phases, resulting in an abrupt reduction in the alloy strength. Such a catastrophic failure is mainly attributed to the presence of large pores, Fig. 20a. It is interesting to note the brittle rupture of the Cu-rich phase particles upon rapid quenching from the molten state (at the interior of the test bars depicted in Fig. 20b).

4. Conclusions

1. Increasing the Mg content in primary A319.2 alloy up to 0.45% enhances considerably the alloy response to heat treatment in the T5 and T6 tempers, more particularly, the T6 temper. In the peak-ageing condition (T5 treatment), the high Mg-containing alloy is seen to possess about 362 MPa (*YS*), 400 MPa (*UTS*), and 1.4% (*El*) compared to 260 MPa (*YS*), 304 MPa (*UTS*), and 1.35% (*El*) reported for the base alloy treated similarly.

2. Modification of the high-Mg version of 319 alloy with Sr in amounts of ∼350 ppm results in a considerable amount of porosity formation which counteracts the beneficial effect of the modification, leading to a noticeable decline in the alloy strength.

3. Grain refining the Sr-modified (A319.2 + 0.45% Mg) alloy produces sounder castings with finer grain sizes. As a result, the alloy exhibits a more or less identical ageing response as that offered by the unmodified (A319.2 + 0.45% Mg) alloy.

4. Addition of Mg in amounts of the order of 0.45% results in the precipitation of $Al_5Mg_8Si_6Cu_2$ phase particles. Modification with Sr tends to cause severe segregation of Cu-containing intermetallics in areas away from the growing Si regions.

5. Solutionizing at 505 °C is characterized by the replacement of the α-aluminium dendritic network with an equiaxed structure. Both Si and Cu-phase particles are segregated into grain boundaries. Due to severe segregation of Cu-phases in Sr-modified alloys, dissolution of the Al_2Cu and $Al_5Mg_8Si_6Cu_2$ phase particles is rather sluggish. Hardening occurs by cooperative precipitation of Al_2Cu and Mg_2Si phase particles.

6. Fracture of intermetallic phases in the interdendritic regions is mostly brittle, with the formation of microcracks at the Si, Cu, Fe-base intermetallics and aluminium interfaces. Fracture of the α-aluminium dendritic network is always ductile as evidenced by the formation of long-sized dimples. However, their size is rather controlled by the type of the heat treatment applied. Ageing the quenched test bars at 150 °C leads to propagation of relatively deep microcracks into the matrix beneath the fracture surface. These cracks are mainly localized in the interdendritic regions.

7. High Mg-containing alloys are sensitive to the solutionizing temperature. Solutionizing at a temperature higher than 505 °C causes incipient melting of Al_2Cu and $Al_5Mg_8Si_6Cu_2$ phases, resulting in an abrupt reduction in the alloy strength.

Acknowledgements

The authors would like to thank Dr. A. M. Samuel for help with the fractography work. Financial support received from the Natural Sciences and Engineering Research Council of Canada, the Fondation de l'Université du Québec à Chicoutimi, and the Centre Québécois de recherche et de développement de l'Aluminium is gratefully acknowledged.

References

1. H. BEUMLER, A. HAMMERSTAD, B. WIETING and R. DASGUPTA, *AFS Trans.* **96** (1988) 1.
2. R. DASGUPTA, C. C. BROWN and S. MAREK, in Proc. Int. Conf. on Molten Aluminium Processing, Orlando, Florida, November 6–7, 1989, p. 31.
3. *Idem., AFS Trans.* **97** (1989) 245.
4. *Idem.*, in Proc. Int. Conf. on Advanced Aluminium and Magnesium Alloys, Orlando, 1990, p. 485.
5. H. DE LA SABLONNIÈRE and F. H. SAMUEL, *Int. J. Cast Metals Res.* **9** (1996) 195.
6. *Idem., ibid.* **9** (1996) 213.
7. J. GAUTHIER and F. H. SAMUEL, *AFS Trans.* **103** (1995) 849.
8. J. GAUTHIER, P. R. LOUCHEZ and F. H. SAMUEL, *Cast Metals* **8** (1995) 91.
9. D. APELIAN, S. SHIVKUMAR and G. SIGWORTH, *AFS Trans.* **97** (1989) 727.
10. P. N. CREPEAU, S. D. ANTOLOVICH and J. A. WORDEN, *ibid.* **98** (1990) 813.
11. J. GAUTHIER, P. R. LOUCHEZ and F. H. SAMUEL, *Cast Metals* **8** (1995) 107.
12. S. SHIVKUMAR, C. KELLER and D. APELIAN, *AFS Trans.* **98** (1990) 905.
13. D. APELIAN, S. SHIVKUMAR and G. SIGWORTH, *ibid.* **97**, (1989) 727.
14. Y. AWANO and Y. SHIMIZU, *ibid.* **98** (1990) 889.
15. A. GANGULEE and J. GURLAND, *Trans. AIME* **239** (1990) 605.
16. E. N. PAN, H. S. CHIOU and G. J. LIAO, *AFS Trans.* **94** (1991) 605.
17. A. M. SAMUEL and F. H. SAMUEL, *Metall. Trans. A* **26A** (1995) 2354.

18. S. SHIVKUMAR, S. RICCI, JR., C. KELLER and D. APELIAN, *J. Heat Treating* **8** (1990) 63.
19. A. M. SAMUEL, P. OUELLET, H. W. DOTY and F. H. SAMUEL, *AFS Trans.* **105** (1997) 951.
20. M. S. MISRA and K. J. OSWALT, *ibid.* **90** (1982) 1.
21. B. KOTTE, Modern Casting, May, 1985, p. 33.
22. "Aluminium: Properties and Physical Metallurgy," (edited by) J. E. Hatch (American Society for Metals, Metals Park, Ohio, 1984) p. 143.
23. L. A. NARAYANAN, F. H. SAMUEL and J. E. GRUZLESKI, *Metall. Mater., Trans. A* **25A** (1996) 1761.
24. A. M. SAMUEL, J. GAUTHIER and F. H. SAMUEL, *ibid.* **27A** (1998) 1785.

Received 9 November 1998
and accepted 15 March 1999